

Evolution of multicellularity coincided with increased diversification of cyanobacteria and the Great Oxidation Event

Bettina E. Schirrmeister^{a,1,2}, Jurriaan M. de Vos^b, Alexandre Antonelli^c, and Homayoun C. Bagheri^a

^aInstitute of Evolutionary Biology and Environmental Studies, University of Zurich, CH-8057 Zurich, Switzerland; ^bInstitute of Systematic Botany, University of Zurich, CH-8008 Zurich, Switzerland; and ^cGothenburg Botanical Garden and Department of Biological and Environmental Sciences, University of Gothenburg, SE 405 30 Gothenburg, Sweden

Edited by Stjepko Golubic, Boston University, Boston, MA, and accepted by the Editorial Board December 13, 2012 (received for review June 15, 2012)

Cyanobacteria are among the most diverse prokaryotic phyla, with morphotypes ranging from unicellular to multicellular filamentous forms, including those able to terminally (i.e., irreversibly) differentiate in form and function. It has been suggested that cyanobacteria raised oxygen levels in the atmosphere around 2.45–2.32 billion y ago during the Great Oxidation Event (GOE), hence dramatically changing life on the planet. However, little is known about the temporal evolution of cyanobacterial lineages, and possible interplay between the origin of multicellularity, diversification of cyanobacteria, and the rise of atmospheric oxygen. We estimated divergence times of extant cyanobacterial lineages under Bayesian relaxed clocks for a dataset of 16S rRNA sequences representing the entire known diversity of this phylum. We tested whether the evolution of multicellularity overlaps with the GOE, and whether multicellularity is associated with significant shifts in diversification rates in cyanobacteria. Our results indicate an origin of cyanobacteria before the rise of atmospheric oxygen. The evolution of multicellular forms coincides with the onset of the GOE and an increase in diversification rates. These results suggest that multicellularity could have played a key role in triggering cyanobacterial evolution around the GOE.

early life | major transitions | prokaryotic phylogenetics | molecular clock

Cyanobacteria are one of the morphologically most diverse groups of prokaryotic organisms. Growth forms range from uni- to multicellular, and can include levels of reversible or terminal (i.e., irreversible) cell differentiation. These diverse growth strategies have enabled cyanobacteria to inhabit almost every terrestrial and aquatic habitat on Earth. Cyanobacteria have traditionally been classified into five subsections according to their morphology (1, 2), where subsections I and II refer to unicellular species and subsections III–V describe multicellular species. Species belonging to subsections IV and V are able to produce terminally differentiated cells. Despite the usefulness of these subsections, molecular evidence shows that morphological and genetic diversity do not always coincide. Molecular phylogenies indicate that probably none of the five subsections is monophyletic (3, 4), and several transitions between uni- and multicellularity have taken place (5). According to the fossil record, various distinct morphotypes attributed to cyanobacteria were already present over 2 billion y ago (Bya) (6, 7). The phylum is thought to have existed as early as 2.45–2.32 Bya, based on the assumption that cyanobacteria were responsible for the accumulation of atmospheric oxygen levels, referred to as the Great Oxidation Event (GOE) (8–12). Despite the generally accepted time-frame for the rise of cyanobacteria, surprisingly little is known about when morphological innovations, such as multicellularity, first appeared. It is also unclear what influence, if any, these innovations may have had on the diversification of the phylum. The assumed link between the rise of atmospheric oxygen and cyanobacteria is also poorly understood: did the GOE closely follow the first appearance of cyanobacteria, or did it take

place considerably later, in possible association with morphological innovations of the phylum?

There have been previous attempts to estimate the origin of cyanobacteria and their morphotypes (13–16). However, it is likely that a biased taxonomic choice, especially missing early branches of the cyanobacterial phylogeny, may have led to incomplete conclusions (17, 18). Phylogenetic evidence indicates that multicellularity evolved very early in the history of cyanobacteria, challenging the view that multicellularity is a derived condition in the phylum (5). Nonetheless, important questions remain: (i) When did cyanobacteria and their major clades evolve? (ii) When did multicellularity first appear? (iii) How are these transitions associated with the GOE around 2.45–2.32 Bya?

The far-reaching impact of the GOE cannot be emphasized enough: it changed Earth's history by enabling the evolution of aerobic life. Unlike other eubacterial phyla, cyanobacteria exhibit a well-studied fossil record (6, 7, 19, 20). However, fossil data are often limited and present only minimum age estimates of clades. Therefore, a combination of fossil data with molecular phylogenetic methods has been advocated (21–23). The use of carefully selected calibration priors for molecular-dating analyses can provide new insights into the temporal evolution of cyanobacteria and the early history of life. Presently, available genome data for cyanobacteria are biased toward unicellular taxa and do not sufficiently represent the known diversity of this phylum. Therefore, we reconstructed phylogenetic trees on the basis of 16S rRNA sequences, which have been carefully sampled based on phylogenetic disparity as described previously (5). We further estimated divergence times of cyanobacteria, and addressed different interpretations of the fossil record as calibration priors. We then evaluated whether the GOE coincided with the development of major cyanobacterial morphotypes present today. Finally, we tested for shifts in diversification rates, incorporating information on 281 species and 4,194 strains. Our results support theories of an early cyanobacterial origin toward the end of the Archean Eon, before 2.5 Bya. Evolution of multicellularity coincided with the onset of the GOE, and corresponded to a marked increase of diversification in cyanobacteria.

Author contributions: B.E.S., J.M.d.V., A.A., and H.C.B. designed research; B.E.S. and J.M.d.V. analyzed data; and B.E.S., J.M.d.V., A.A., and H.C.B. wrote the paper.

The authors declare no conflict of interest.

This article is a PNAS Direct Submission. S.G. is a guest editor invited by the Editorial Board.

Freely available online through the PNAS open access option.

Data deposition: The sequences reported in this paper have been deposited in the GenBank database (accession no. [JX069960](#)).

¹Present address: School of Earth Sciences, University of Bristol, Bristol BS8 1RJ, United Kingdom.

²To whom correspondence should be addressed. E-mail: bettina.schirrmeister@bristol.ac.uk.

This article contains supporting information online at www.pnas.org/lookup/suppl/doi:10.1073/pnas.1209927110/-DCSupplemental.

Results

Phylogenetic Analyses. To infer the early evolution of cyanobacteria, we reconstructed Bayesian phylogenetic trees using 16S rRNA sequence data. A phylogenomic approach would give misleading results, because available cyanobacterial genome sequences, to date, are heavily biased toward unicellular species. Moreover, the few multicellular species that have been fully sequenced are phylogenetically closely related, and a comparison of these species is unlikely to provide any information on the ancient origin of multicellularity in cyanobacteria (17). In a previous study (5), a phylogenetic tree of 1,220 cyanobacterial sequences was reconstructed from which a subset of taxa was sampled that represents the surveyed diversity of this phylum. Here we used this subset plus one strain (G40) that represents a potentially unique distinct species isolated by our group. Our unconstrained phylogenetic results (Fig. S1) agree with previous findings (3, 5, 15, 24, 25), which reject monophyly of several morphological groups previously described (1, 2). Furthermore, *Gloeobacter violaceus* is resolved as the sister group of all other cyanobacteria. Three major groups can be distinguished (clades E1, E2, and group AC) (Fig. 1, and Figs. S1 and S2), together representing the majority of cyanobacterial taxa living today. All

groups have been defined previously (5), with clades E1 and E2 (subclades of E) including species of all morphological subsections. Species belonging to morphological subsections IV and V occur solely in E1. The group AC contains unicellular marine pico-phytoplankton (subsection I) as well as some undifferentiated multicellular species (subsection III).

Divergence Time Estimation. Divergence times along the cyanobacterial phylogeny were estimated under Bayesian relaxed molecular clocks using two different models of uncorrelated rate evolution (26). A lognormal distribution of rates has been shown to outperform a model with exponential rate distribution (26). Therefore, our first model assumed rates were lognormally distributed (uncorrelated lognormal, UCLN). Robustness of results was tested with a second model assuming exponentially distributed rates (uncorrelated exponentially distributed, UCED) (SI Text). For each clock model a set of eight different analyses were performed to take a broad range of prior assumptions into account and evaluate their influence on the results (Table 1 and Table S1). The Bayesian consensus tree of divergence-time analysis 7 is presented in Fig. 1, including age estimates (95% highest posterior densities, HPD) of important nodes as given by

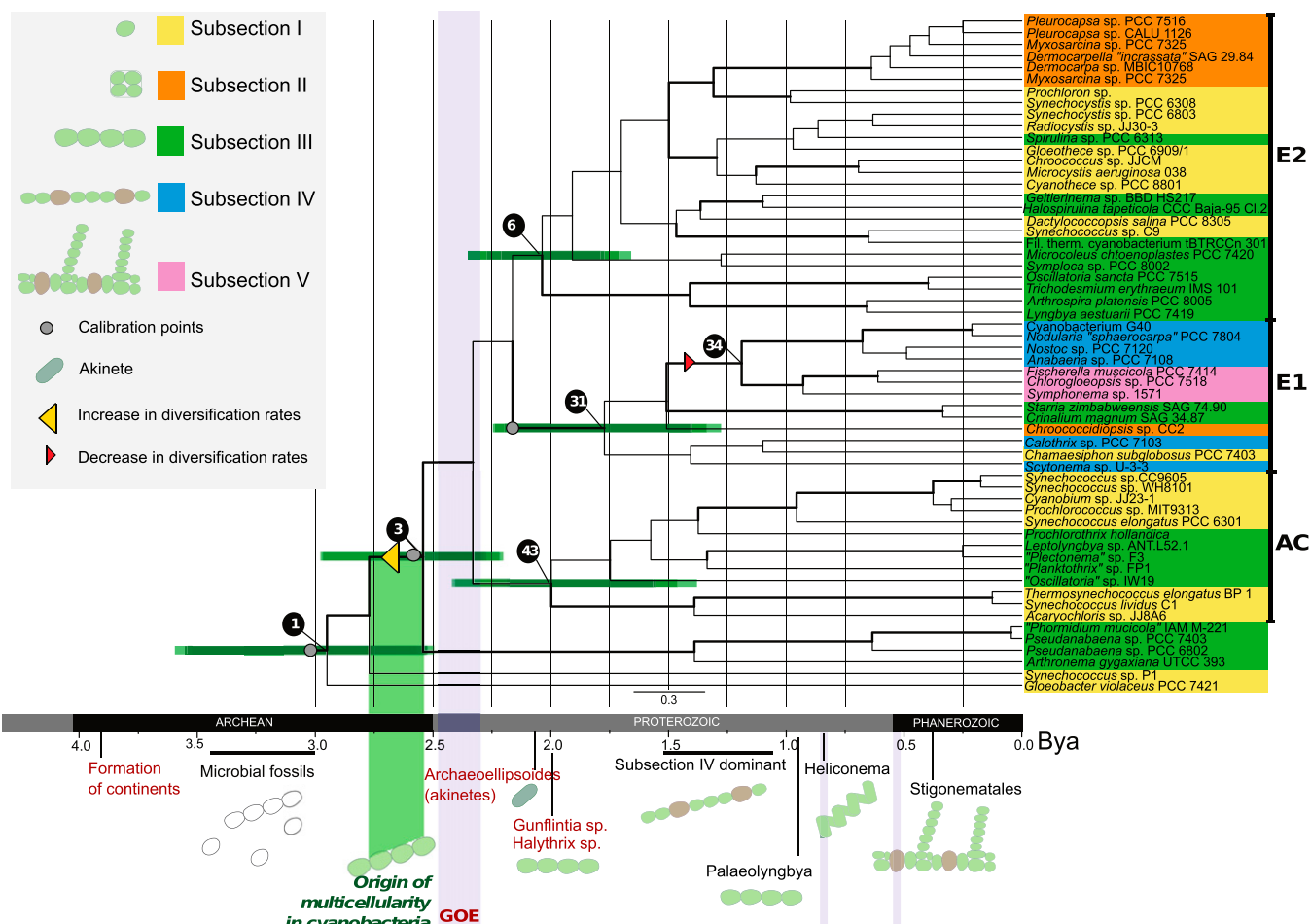


Fig. 1. Time calibrated phylogeny of cyanobacteria displaying divergence time estimates. Bayesian consensus tree (analysis 7) based on 16S rRNA data with 95% highest posterior densities of the discussed node ages shown as green bars (analyses 1, 3, 5, and 7 overlapping). Morphological features of taxa are marked by colored boxes and listed in the inset. Full taxon names are displayed in Table S3. Branches with posterior probabilities >0.9 in all analyses are presented as thick lines. Gray circles mark points used for calibration of the tree. Details of the prior age estimates used for calibration are presented in Table 1. A significant increase in diversification rate (yellow triangle) [9.66-fold (average of all analyses)] can be detected at node 3 and a minor decrease (red triangle) at 33/34. The earlier shift close to node 3 coincides with the origin of multicellularity. Schematic drawings of cyanobacterial fossils are provided under the timeline, with the ones used for calibration of the tree marked in red. Our results indicate that multicellularity (green shade) originated before or at the beginning of the GOE.

Table 1. Divergence times for five important nodes estimated using a relaxed clock with UCLN distributed evolutionary rates

Analysis	1	2	3	4	5	6	7	8
Model assumptions and calibration points								
Outgroup	No	—	Yes	Yes	Yes	Yes	Yes	No
Root	—	LN(2,1;2,27,0,5)	Exp(2,45;2,816)*	Exp(2,45;2,816)*	Exp(2,45;2,816)*	Exp(2,45;2,816)*	Exp(2,45;2,816)*	*
Node 3	LN(2,1;2,27,0,5)	LN(2,1;2,58,0,8)	LN(2,1;2,27,0,5)	LN(2,1;2,58,0,8)	LN(2,1;2,27,0,5)	LN(2,1;2,58,0,8)	LN(2,1;2,27,0,5)	LN(2,1;2,58,0,8)
Node 31 or 32	LN(2,1;2,13,1)							
Results for discussed nodes (UCLN) (\tilde{m}) (HPD) for all								
Node 1	2.95 (2.5–3.6)	3.67 (2.79–4.74)	2.99 (2.57–3.55)	3.35 (2.74–4.15)	2.87 (2.53–3.30)	3.06 (2.66–3.53)	2.95 (2.53–3.55)	3.39 (2.87–3.80)
Node 3	2.54 (2.28–2.98)	3.08 (2.42–3.84)	2.42 (2.21–2.73)	2.65 (2.28–3.18)	2.38 (2.20–2.62)	2.49 (2.26–2.81)	2.54 (2.29–2.97)	2.86 (2.43–3.34)
Node 6	2.04 (1.77–2.35)	2.33 (1.89–2.87)	2.02 (1.72–2.28)	2.10 (1.78–2.54)	1.99 (1.67–2.22)	2.02 (1.70–2.32)	2.04 (1.79–2.35)	2.18 (1.86–2.60)
Node 31	1.77 (1.4–2.24)	2.16 (1.53–2.56)	1.72 (1.34–2.20)	1.98 (1.39–2.34)	1.67 (1.28–2.17)	1.75 (1.30–2.23)	1.77 (1.41–2.25)	2.12 (1.50–2.41)
Node 43	2.00 (1.56–2.43)	2.35 (1.73–3.03)	1.85 (1.46–2.25)	1.97 (1.48–2.50)	1.80 (1.38–2.19)	1.86 (1.41–2.30)	2.00 (1.57–2.41)	2.18 (1.71–2.72)

Eight different combinations of calibration priors for the divergence time estimation were used. Exp, exponential distribution (offset;mean); LN, lognormal distribution (offset;mean); SD, —, calibration not applicable.
*Truncated at 3.8 Bya.

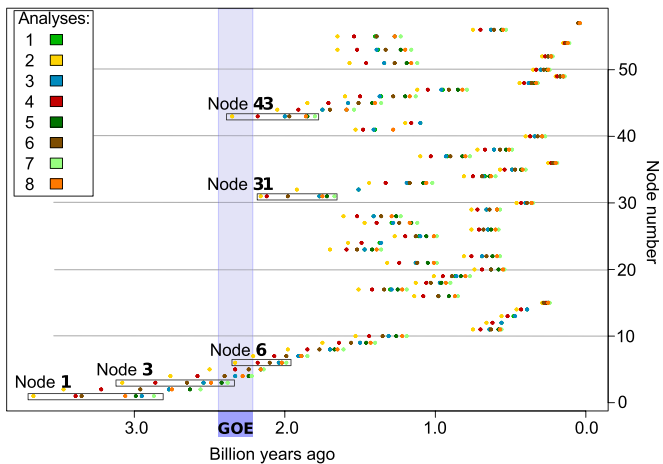


Fig. 2. Median age estimates under eight analytical scenarios. Median age estimates of clades (Table 1). The origin of cyanobacteria (node 1) and the evolution of multicellularity (node 3) are estimated before or at the beginning of the GOE. Relatively soon after the GOE, the stem lineages of the three major cyanobacterial clades originated, containing unicellular cyanobacteria (node 6), terminally differentiated taxa (node 31), and marine phytoplankton (node 43).

analyses 1, 3, 5, and 7 (Table 1). Median node ages (\tilde{m}) are shown in Fig. 2, and are provided with 95% HPD in Table 1 (discussed nodes) and Table S2 (all nodes). Although ages of cyanobacterial nodes varied with respect to the analyses, our major conclusions are robust to different calibration priors. All analyses indicated that extant cyanobacteria originated before the GOE (2.45 Bya). Multicellularity most likely originated along the branch leading to node 3 (5). For this node, analyses suggested a median age before or at the beginning of the GOE (before 2.36 Bya) (Table 1 and Table S1). The ancestor of the lineage leading to node 3 was also a calibration point in our analyses (Table 1). Fig. 3 compares the implied prior probability distributions of that calibration point to posterior probabilities of node 3, hence assessing the extent to which our prior assumptions affected the outcome. Although the prior assumptions put a higher probability on an age after the GOE around 2.2 Bya, our data contained strong signals to counteract these priors and indicate instead an older median node age for node 3, between 2.42–3.08 Bya (all analyses) (Fig. 3 and Table 1), which is before the GOE. Furthermore, groups E1, E2, and AC are estimated to have originated around the end of the GOE. These groups comprise the majority of living cyanobacteria (91% of 281 species and 88% of 4,194 strains).

Shifts in Diversification Rates. To identify whether the GOE or multicellularity might have influenced the net diversification of cyanobacteria, we tested whether diversification rates have been constant among cyanobacterial lineages. Because previous work suggested that taxonomy of cyanobacteria needed revision (1), we ran analyses incorporating information on both species (281) and strains (4,194). Clades containing many species also contain many strains (Table S3). Results from the diversification rate estimation showed similar patterns independent of whether species numbers or strain numbers were used (Table S4). Two significant shifts in diversification rates were detected. At node 3/4, where multicellularity evolved, the diversification rate increased on average 8.44-fold (SD = 1.76) for trees reconstructed with a UCLN model and 5.24-fold (SD = 1.89) for trees reconstructed with a UCED model (averaged over all analyses) (Table S4). Subsequently, at node 33/34, the diversification rate decreased by a factor of 0.55 (SD = 0.19) for trees reconstructed with a

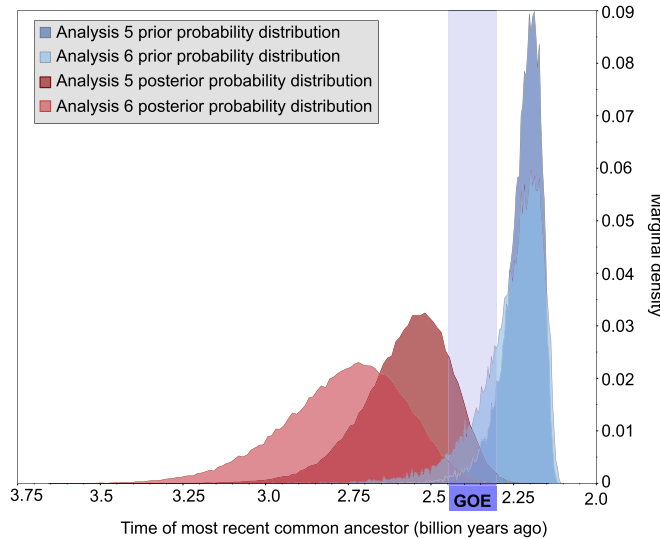


Fig. 3. Prior and posterior probability distributions of ages for node 3. Marginal prior probability distributions of analyses using narrow (analysis 5) and wide (analysis 6) prior distributions were conservatively biased toward younger ages, strongly favoring an origin of multicellularity after the GOE. Even so, posterior probabilities point to an origin of multicellularity before or at the beginning of the GOE, indicating that this main result is based on a strong signal in the data rather than a bias from a-priori assumptions. Marginal prior probability distributions were estimated in analyses that only sampled from the prior.

UCLN model, and by a factor of 0.22 (SD = 0.13) for trees reconstructed with a UCED model (Fig. 1 and Figs. S3–S6).

Discussion

Limitations of a Single Gene. The exchange of genetic material across species boundaries poses a challenge for the inference of evolutionary histories of living organisms (27–29). Phylogenetic reconstructions incorporating multiple genes help to reduce the danger to recover false signals from genes affected by horizontal gene transfer (HGT) (30, 31). Nevertheless, although genome data are accumulating, they do not nearly achieve the breadth of microbial diversity represented by 16S rRNA (32). 16S rRNA has been used as a reliable measure of phylogenetic relationship because of its size and conservation (33, 34, 35). These facts, in combination with a potentially smaller impact of HGT on genome evolution than commonly assumed, and even less on 16S rRNA (32, 36, 37), support the usefulness of the small ribosomal subunit for phylogenetic applications. Here we can neither exclude nor prove the possibility of 16S rRNA being affected by HGT between species. No cases have been found in support of HGT for 16S rRNA between cyanobacterial genera. We rely on 16S rRNA sequences in this study because a genomic approach would be biased toward unicellular taxa, would not cover the complete known diversity of this phylum and, hence, fail to reconstruct the early evolution of cyanobacteria (17). Nevertheless, we strongly encourage genome-sequencing projects that will help to recover the diversity indicated by 16S rRNA and improve reconstruction of a cyanobacterial phylogeny.

Evolution of Multicellularity and Possible Consequences. In prokaryotes simple forms of multicellularity occur in different phyla. In Actino- and Myxobacteria, multicellular growth formed via cell aggregation is part of their life cycle (38). In cyanobacteria, chloroflexi, and some proteobacteria (e.g., *Beggiatoa*) multicellularity is in a filamentous form. This result is achieved through cell division and adhesion, which results in filament elongation (39). Requirements for directed growth in filaments are cellular recognition of polarity (40) and cellular communication. Filamentous cyanobacteria,

including simple forms like *Pseudanabaena* and *Leptolyngbya*, show directional growth where the plane of cell division depicts a right angle to the growth direction (1). In addition, intercellular communication and resource exchange has been found in cyanobacteria (41–43), providing an evolutionary basis for the division of labor and terminal cell differentiation to evolve (44–46).

Our results suggest a concurrence of the origin of multicellularity, the onset of the GOE, and an increased diversification rate of cyanobacteria; in addition, although their precise timing cannot be fully ascertained, they can be linked by theoretical and empirical lines of evidence. The transition to multicellularity represents an important change in organic complexity (47). There are various advantages that multicellularity could confer (39, 48). Among others, filamentous growth can improve motility (49), and cooperation of cells may also increase fitness because of economies of scale. Experimental studies have shown that multicellularity might evolve relatively fast given selective pressure (50) and can provide metabolic fitness advantages compared with single cells (51). Increased fitness of multicellular species could have led to a higher frequency and wider distribution of cyanobacteria at the end of the Archean, consequently enhancing oxygen production. Accumulation of oxygen may have resulted in new ecological opportunities. Increased diversification rates around the time when multicellularity evolved suggest that cyanobacteria might have used, and possibly contributed to create, new adaptive opportunities. Subsequently, at the end of the GOE, three clades (E1, E2, and AC) evolved that led to the majority of cyanobacteria living today.

Early Earth History and the Fossil Record. Our finding that cyanobacteria have existed for a longer time than previously anticipated is congruent with reconstructions of early Earth history. The origin of Earth is deduced to date back ~4.5 Bya (52). Subsequently, the planet cooled down and eventually separated into core, mantle, and crust (53). Permanent existence of life before 4.2–3.8 Bya is unlikely, considering that the young Earth was subject to strong bombardment by asteroids (52, 54). Fossil evidence does not predate ~3.45 Bya (55, 56). Most of these prokaryotic fossils from the early Archean Eon have been identified in two regions: the Barberton Greenstone Belt (BGB), South Africa (around 3.20–3.50 billion y old), and the Pilbara Craton (PC), Western Australia (around 2.90–3.60 billion y old) (55–60). The oldest fossils from these regions are spherical, probably hyperthermophilic microbes [BGB (56, 59)] and filaments of possibly anoxygenic photosynthetic prokaryotes [East-PC (55, 56)], both around 3.45 billion y old. Further evidence for life includes 3.4 billion-y-old trace fossils (PC) (60), 3.42 billion-y-old deformed microbial mats (BGB) (57), and 3.0 billion-y-old biofilms (PC) (58). The earliest unequivocal cyanobacterial fossils date back around 2.0 Bya and come from two localities, the Gunflint iron formation and the Belcher Subgroup (both in Canada) (19, 20). Although differences in the microbial fossil composition have been recognized (19), both cherts include filamentous and coccoidal species. *Gunflintia grandis* and *Gunflintia minuta* have been identified as filamentous cyanobacterial fossils from the Gunflint iron formation, and *Halythrix* sp. has been described as an oscillatorian fossil from the Belcher subgroup (7) (Fig. 1). Cyanobacterial fossils younger than 2 billion y are more widely distributed (20), with various examples given in Fig. 1. Archean fossil findings may potentially depict remains of cyanobacteria but cannot be assigned beyond doubt (20). “Possible” cyanobacterial fossils have been found in 2.52–2.55 billion-y-old cherts in South Africa (20, 61). “Probable” unicellular and filamentous cyanobacterial fossils are distributed in 2.6 billion-y-old (20, 62–64) and 3.26 billion-y-old (64) cherts. Although previously described biomarkers that supported an existence of cyanobacteria around 2.7 Bya (65, 66) have been dismissed (67), recent evidence has been found in favor of an early cyanobacterial origin

(68–70). Our molecular dating results place the origin of both unicellular and multicellular cyanobacteria rather before the GOE, and thus suggest that some of those fossils could indeed represent relatives of cyanobacterial lineages.

Recent studies have suggested that oxygen accumulation occurred ~200–300 million y before the GOE (68, 69, 71). Current evidence from the fossil record, geochemical findings, and our molecular analyses, together support an origin of cyanobacteria clearly before the GOE. The origin of multicellularity toward the GOE could have entailed fitness advantages leading to an increase in cyanobacterial diversity and abundance, which in turn would positively influence net oxygen production.

Conclusion

Cyanobacteria are one of the morphologically most diverse prokaryotic phyla on this planet. It is widely accepted that they caused the GOE starting 2.45 Bya, but debates about their origin are still ongoing (67, 72, 73). Various lines of fossil and geochemical evidence have accumulated, supporting an origin of cyanobacteria before 2.45 Bya (20, 62, 64, 68–70). Here, we applied Bayesian phylogenetic analyses using relaxed molecular clocks and different combinations of calibration priors. We estimated the origin of extant cyanobacteria and their dominant morphotypes with respect to the GOE. Although resulting age estimates of the different analyses differ somewhat in their HPD, robust statements regarding the origin of cyanobacteria and their morphotypes can nevertheless be formulated: (i) cyanobacteria originated before the GOE, (ii) multicellularity coincides with the beginning of the rise of oxygen, and (iii) three clades representing the majority of extant cyanobacteria evolved shortly after the accumulation of atmospheric oxygen.

Materials and Methods

Taxon Sampling. Most sequences were downloaded from GenBank (74) (Table S3). Three eubacterial species were chosen as an outgroup: *Beggiaota* sp., *Chlamydia trachomatis*, and *Spirochaeta thermophila*. A total of 58 cyanobacterial species were chosen for the analyses. Aside from strain G40 (SI Text) all taxa were selected as described previously (5). The taxa chosen comprise all morphological subsections described by Castenholz (1) and cover the morphological and genetic diversity of this phylum (5). Nomenclature and identity stated on GenBank might be incorrect. Therefore, we evaluated morphotypes (multicellular/unicellular) of each cyanobacterial strain by thoroughly examining the literature (Table S5) and conducting BLAST analyses, as described in SI Text. For most of those situations, full genome data are not yet available (17).

Alignment and Divergence Time Estimation. Sequence alignments were constructed using the program MUSCLE (Dataset S1) (75). Analyses were performed on datasets with outgroups [(i) 61 taxa, 1,090 sites, gaps excluded; 507 sites variable] and without outgroups [(ii) 58 taxa, 1,077 sites, gaps excluded; 421 sites variable]. Uncorrected and corrected Akaike Information Criterion (76, 77), implemented in jModelTest v0.1.1 (78), suggested a general time-reversible substitution model with γ -distributed rate variation among sites (GTR+G) (79) as the most suitable model of sequence evolution. Phylogenetic analyses using Bayesian inference were conducted as described in SI Text. We applied relaxed clocks with UCLN and UCED rate distributions (Table 1 and Table S1) (80). The analyses were conducted with a combination of three calibration points. Additionally, monophlyy constraints were set for three nodes that were supported by our previous Bayesian phylogenetic analyses (Fig. S1 and SI Text): (i) the phylum cyanobacteria, (ii) cyanobacteria, excluding *Gloeobacter*, and (iii) cyanobacteria excluding *Synechococcus* sp. P1 and *Gloeobacter* (Fig. 1). The phylum cyanobacterian (i) has been extensively investigated and confirmed before [i.e., cyanobacteria as a monophyletic group within the Eubacteria (5)]. For cyanobacteria, excluding *Gloeobacter* (ii), an early divergence of *Gloeobacter* has been supported in previous analyses (5, 17, 24). Unlike other cyanobacteria, *G. violaceus* lacks

thylacoid membranes (81), and various differences in gene content compared with cyanobacteria have been found (82). For cyanobacteria excluding *Synechococcus* sp. P1 and *Gloeobacter* (iii), *Synechococcus* sp. P1 is a thermophilic unicellular cyanobacterium isolated from Octopus Spring in Yellowstone national park (83). Its proximity to *Gloeobacter* and eubacterial outgroups has been shown by genetic comparisons and phylogenetic analyses (5, 17, 24). Divergence time estimation was conducted using the software BEAST v1.6.2 (80) and run on the CIPRES Science Gateway v.3.1 (84). For each analysis, we ran six Markov chain Monte Carlo chains for 50-million generations, sampling every 2,000th generation (input files provided as Dataset S2). Although convergence of all parameters was reached before 5 million generations, we excluded a conservative 25% initial burn-in. Results are presented on a 50% majority-rule consensus tree calculated with SumTrees v3.3.1 (85).

Calibration Points. The root: Stem lineage of cyanobacteria. Four of the eight divergence time analyses included an outgroup (Table 1: analyses 3, 4, 5, 6), which enabled calibrating the cyanobacterial stem lineage. The GOE dates back 2.32–2.45 billion y (9), and is assumed to be a result of cyanobacterial activity. We use the start of the GOE as the minimum date for the divergence of cyanobacterial stem lineage and the outgroup. The possibility of permanently existing lifeforms is suggested to occur earliest around 3.8 Bya (52), which we used as earliest date (i.e., maximum age) of our root calibration. See Table 1 for a detailed description of prior age probability distributions. For analyses 7 and 8, the age of the earliest split of cyanobacteria, namely between *Gloeobacter* and the rest of cyanobacteria, was accordingly restricted to 3.8–2.45 Bya.

Node 3: First multicellular cyanobacteria. Node 3 in Fig. 1 was estimated to be a multicellular ancestor of extant cyanobacteria, as recovered previously (5). Fossil records indicate that terminally differentiated cyanobacteria (subsections IV and V) evolved before 2.1 Bya. Such differentiation may only evolve in a multicellular setting (44). We therefore assume that the stem lineage of node 3 must have been present before 2.1 Bya, and use this as a hard minimum bound of a lognormal prior distribution. We used a soft upper bound, linking the distribution of prior probabilities to the timing of the GOE. Multicellularity may have evolved as a consequence of new habitats that became available after the GOE, 2.3 Bya, or it could instead have triggered a rise of oxygen in the atmosphere. Therefore, we distinguish two calibration scenarios, one by setting the probability of the age of node 3 to a lognormal distribution with 95% being younger than 2.45 (Table 1: analyses 1, 3, 5), and the other by setting the median age of the before 2.45 Bya (Table 1: analyses 2, 4, 6).

Node 31 or 32: First terminally differentiated cyanobacteria. Cyanobacteria belonging to subsection IV and V share the property to form resting cells named akinetes. Fossilized remains of these akinetes have been identified at various locations throughout the Proterozoic (6, 19, 86). The oldest of these fossilized akinetes are found in 2.1 billion-y-old rocks (6, 13), and imply that cyanobacteria belonging to subsection IV and V originated before 2.1 Bya. Taxa of this group are capable of terminal cell differentiation. Oxygen sensitive nitrogen fixation is spatially separated from oxygenic photosynthesis and takes place in so called heterocysts. Oxygen levels providing a selective advantage for separation of these processes were reached ~2.45 Bya (13). As a calibration for the divergence time estimation, we set the most recent common ancestor of taxa from subsections IV and V to 2.1 billion y as a hard minimum bound, and specified 95% of prior probabilities before 2.45 Bya, using a lognormal distribution.

Shifts in Diversification Rates. To test whether the rate of lineage accumulation has been constant throughout cyanobacterial evolution, we used the function MEDUSA from the geiger 1.3-1 package in R (87). We corrected for possible taxon sampling biases by including information on known numbers of extant species and strains, which were collected from GenBank. Details are given in SI Text and Table S3. MEDUSA was run based on 50% majority-rule consensus trees calculated with SumTrees v3.3.1 (85), derived from the eight BEAST analyses (Table 1).

ACKNOWLEDGMENTS. We thank Akos Dobay, Valentina Rossetti, Manuela Filippini-Cattani, the editor S.G., and three anonymous reviewers for helpful comments on the manuscript. This work was supported in part by Canton of Zurich; A.A. is supported by grants from the Swedish and the European Research Councils. B.E.S. is supported by the Swiss National Science Foundation.

- Boone DR, Castenholz RW (2001) *Bergey's Manual of Systematic Bacteriology: The Archaea and the Deeply Branching and Phototrophic Bacteria: Cyanobacteria*, ed Garrity GM (Springer, New York).
- Rippka R, Deruelles J, Waterbury JB, Herdman M, Stanier RY (1979) Generic assignments, strain histories and properties of pure cultures of cyanobacteria. *J Gen Microbiol* 111: 1–61.

- Giovannoni SJ, et al. (1988) Evolutionary relationships among cyanobacteria and green chloroplasts. *J Bacteriol* 170(8):3584–3592.
- Gugger MF, Hoffmann L (2004) Polyphly of true branching cyanobacteria (Stigonimates). *Int J Syst Evol Microbiol* 54(Pt 2):349–357.
- Schirrmeyer BE, Antonelli A, Bagheri HC (2011) The origin of multicellularity in cyanobacteria. *BMC Evol Biol* 11:45.

6. Amard B, Bertrand-Sarfati J (1997) Microfossils in 2000 ma old cherty stromatolites of the Franceville group, Gabon. *Precambrian Res* 81(3–4):197–221.
7. Hofmann HJ (1976) Precambrian Microflora, Belcher islands, Canada—Significance and systematics. *J Paleonto* 50(6):1040–1073.
8. Blankenship RE (2002) *Molecular Mechanisms of Photosynthesis* (Blackwell Science, Oxford).
9. Bekker A, et al. (2004) Dating the rise of atmospheric oxygen. *Nature* 427(6970):117–120.
10. Kopp RE, Kirschvink JL, Hilburn IA, Nash CZ (2005) The Paleoproterozoic snowball Earth: A climate disaster triggered by the evolution of oxygenic photosynthesis. *Proc Natl Acad Sci USA* 102(32):11131–11136.
11. Allen JF, Martin W (2007) Evolutionary biology: Out of thin air. *Nature* 445(7128):610–612.
12. Frei R, Gaucher C, Poulton SW, Canfield DE (2009) Fluctuations in Precambrian atmospheric oxygenation recorded by chromium isotopes. *Nature* 461(7261):250–253.
13. Tomitani A, Knoll AH, Cavanaugh CM, Ohno T (2006) The evolutionary diversification of cyanobacteria: Molecular-phylogenetic and paleontological perspectives. *Proc Natl Acad Sci USA* 103(14):5442–5447.
14. Battistuzzi FU, Hedges SB (2009) A major clade of prokaryotes with ancient adaptations to life on land. *Mol Biol Evol* 26(2):335–343.
15. Blank CE, Sánchez-Baracaldo P (2010) Timing of morphological and ecological innovations in the cyanobacteria—A key to understanding the rise in atmospheric oxygen. *Geobiology* 8(1):1–23.
16. Larsson J, Nylander JAA, Bergman B (2011) Genome fluctuations in cyanobacteria reflect evolutionary, developmental and adaptive traits. *BMC Evol Biol* 11:187.
17. Schirrmeister BE, Anisimova M, Antonelli A, Bagheri HC (2011) Evolution of cyanobacterial morphotypes: Taxa required for improved phylogenomic approaches. *Commun Integr Biol* 4(4):424–427.
18. Wu DY, et al. (2009) A phylogeny-driven genomic encyclopaedia of Bacteria and Archaea. *Nature* 462(7276):1056–1060.
19. Golubic S, Lee SJ (1999) Early cyanobacterial fossil record: Preservation, palaeoenvironments and identification. *Eur J Phycol* 34(4):339–348.
20. Sergeev VN, Gerasimenko LM, Zavarzin GA (2002) [Proterozoic history and present state of cyanobacteria]. *Mikrobiologiya* 71(6):725–740.
21. Benton MJ (2003) The quality of the fossil record. *Telling the Evolutionary Time: Molecular Clocks and the Fossil Record*, eds Donoghue PCJ, Smith MP (Tayler & Francis, London), pp 66–90.
22. Reisz RR, Müller J (2004) Molecular timescales and the fossil record: A paleontological perspective. *Trends Genet* 20(5):237–241.
23. Donoghue PCJ, Benton MJ (2007) Rocks and clocks: Calibrating the Tree of Life using fossils and molecules. *Trends Ecol Evol* 22(8):424–431.
24. Turner S, Pryer KM, Miao VPW, Palmer JD (1999) Investigating deep phylogenetic relationships among cyanobacteria and plastids by small subunit rRNA sequence analysis. *J Eukaryot Microbiol* 46(4):327–338.
25. Honda D, Yokota A, Sugiyama J (1999) Detection of seven major evolutionary lineages in cyanobacteria based on the 16S rRNA gene sequence analysis with new sequences of five marine *Synechococcus* strains. *J Mol Evol* 46(6):723–739.
26. Drummond AJ, Ho SYW, Phillips MJ, Rambaut A (2006) Relaxed phylogenetics and dating with confidence. *PLoS Biol* 4(5):e88.
27. Doolittle WF (1999) Phylogenetic classification and the universal tree. *Science* 284 (5423):2124–2129.
28. Gogarten JP, Doolittle WF, Lawrence JG (2002) Prokaryotic evolution in light of gene transfer. *Mol Biol Evol* 19(12):2226–2238.
29. Andam CP, Gogarten JP (2011) Biased gene transfer in microbial evolution. *Nat Rev Microbiol* 9(7):543–555.
30. Suchard MA (2005) Stochastic models for horizontal gene transfer: Taking a random walk through tree space. *Genetics* 170(1):419–431.
31. Lapierre P, Lasek-Nesselquist E, Gogarten JP (2012) The impact of HGT on phylogenetic reconstruction methods. *Brief Bioinform*, 10.1093/bib/bbs050.
32. Yarza P, et al. (2008) The All-Species Living Tree project: A 16S rRNA-based phylogenetic tree of all sequenced type strains. *Syst Appl Microbiol* 31(4):241–250.
33. Woese CR (1987) Bacterial evolution. *Microbiol Rev* 51(2):221–271.
34. Olsen GJ, Woese CR (1993) Ribosomal RNA: A key to phylogeny. *FASEB J* 7(1):113–123.
35. Schirrmeister BE, Dalquen DA, Anisimova M, Bagheri HC (2012) Gene copy number variation and its significance in cyanobacterial phylogeny. *BMC Microbiol* 12(1):177.
36. Snell B, Bork P, Huynen MA (2002) Genomes in flux: The evolution of archaeal and proteobacterial gene content. *Genome Res* 12(1):17–25.
37. Kurland CG, Canback B, Berg OG (2003) Horizontal gene transfer: A critical view. *Proc Natl Acad Sci USA* 100(17):9658–9662.
38. Rokas A (2008) The molecular origins of multicellular transitions. *Curr Opin Genet Dev* 18(6):472–478.
39. Rossetti V, Filippini M, Svercel M, Barbour AD, Bagheri HC (2011) Emergent multicellular life cycles in filamentous bacteria owing to density-dependent population dynamics. *J R Soc Interface* 8(65):1772–1784.
40. Knoll AH, Javaux EJ, Hewitt D, Cohen P (2006) Eukaryotic organisms in Proterozoic oceans. *Philos Trans R Soc Lond B Biol Sci* 361(1470):1023–1038.
41. Giddings TH, Staehelin LA (1981) Observation of Micromesismata in both heterocyst-forming and non-heterocyst forming filamentous Cyanobacteria by freeze-fracture electron microscopy. *Arch Microbiol* 129(4):295–298.
42. Flores E, Herrero A, Wolk CP, Maldener I (2006) Is the periplasm continuous in filamentous multicellular cyanobacteria? *Trends Microbiol* 14(10):439–443.
43. Flores E, Herrero A (2010) Compartmentalized function through cell differentiation in filamentous cyanobacteria. *Nat Rev Microbiol* 8(1):39–50.
44. Rossetti V, Schirrmeister BE, Bernasconi MV, Bagheri HC (2010) The evolutionary path to terminal differentiation and division of labor in cyanobacteria. *J Theor Biol* 262(1):23–34.
45. Ispolatov I, Ackermann M, Doebeli M (2012) Division of labour and the evolution of multicellularity. *Proc Biol Sci* 279(1734):1768–1776.
46. Rossetti V, Bagheri HC (2012) Advantages of the division of labour for the long-term population dynamics of cyanobacteria at different latitudes. *Proc Biol Sci* 279(1742):3457–3466.
47. Maynard Smith J, Szathmary E (1995) *The Major Transitions in Evolution*. (Oxford University Press, Oxford).
48. Bonner J (1998) The origin of multicellularity. *Integr Biol* 1(1):28–36.
49. Adams DG (1997) *Cyanobacteria. Bacteria as Multicellular Organism*, eds Shapiro JA, Dworkin M (Oxford Univ Press, New York), pp 109–148.
50. Ratcliff WC, Denison RF, Borrello M, Travisano M (2012) Experimental evolution of multicellularity. *Proc Natl Acad Sci USA* 109(5):1595–1600.
51. Koschwanez JH, Foster KR, Murray AW (2011) Sucrose utilization in budding yeast as a model for the origin of undifferentiated multicellularity. *PLoS Biol* 9(8):e1001122.
52. Nisbet EG, Sleep NH (2001) The habitat and nature of early life. *Nature* 409(6823):1083–1091.
53. Mojzsis SJ (2010) Early earth leftover lithosphere. *Nat Geosci* 3:148–149.
54. Sleep NH, Zahnle KJ, Kasting JF, Morowitz HJ (1989) Annihilation of ecosystems by large asteroid impacts on the early Earth. *Nature* 342(6246):139–142.
55. Westall F, et al. (2006) The 3.466 ga “Kitty’s gap chert” an early Archean microbial ecosystem. *Spec Pap Geol Soc Am* 405:105–131.
56. Wacey D (2009) *Early Life on Earth: A Practical Guide* (Springer, New York).
57. Tice MM, Lowe DR (2004) Photosynthetic microbial mats in the 3,416-Myr-old ocean. *Nature* 431(7008):549–552.
58. Sugitani K, et al. (2007) Diverse microstructures from Archaean chert from the mount Goldsworthy-mount grant area, Pilbara Craton, Western Australia: Microfossils, du-biofossils, or pseudofossils? *Precambrian Res* 158:228–262.
59. Glikson M, et al. (2008) Microbial remains in some earliest Earth rocks: Comparison with a potential modern analogue. *Precambrian Res* 164(3–4):187–200.
60. Wacey D, et al. (2008) Use of nanosims in the search for early life on Earth: Ambient inclusion trails in a c. 3400 ma sandstone. *J Geol Soc London* 165(1):43–53.
61. Knoll AH (1996) *Palynology: Principles and Applications—Archean and Proterozoic Paleontology*. (American Association of Stratigraphic Palynologists, Tulsa, OK), pp 51–80.
62. Alterman W, Schopf JW (1995) Microfossils from the Neorachean Campbell Group, Griqualand west sequence of the Transvaal Supergroup, and their paleoenvironmental and evolutionary implications. *Precambrian Res* 75(1–2):65–90.
63. Kazmierczak J, Alterman W (2002) Neorachean biomineralization by benthic cyanobacteria. *Science* 298(5602):2351.
64. Schopf JW (2009) Paleontology, microbial. *Encyclopedia of Microbiology*, eds Lederberg J, Schaechter M (Elsevier, Amsterdam), 3rd Ed, pp 390–400.
65. Brocks JJ, Logan GA, Buick R, Summons RE (1999) Archean molecular fossils and the early rise of eukaryotes. *Science* 285(5430):1033–1036.
66. Summons RE, Jahnke LL, Hope JM, Logan GA (1999) 2-Methylhopanoids as biomarkers for cyanobacterial oxygenic photosynthesis. *Nature* 400(6744):554–557.
67. Rasmussen B, Fletcher IR, Brocks JJ, Kilburn MR (2008) Reassessing the first appearance of eukaryotes and cyanobacteria. *Nature* 455(7216):1101–1104.
68. Lyons TW, Reinhard CT (2011) Earth science: Sea change for the rise of oxygen. *Nature* 478(7368):194–195.
69. Gaillard F, Scaillet B, Arndt NT (2011) Atmospheric oxygenation caused by a change in volcanic degassing pressure. *Nature* 478(7368):229–232.
70. Waldbauer JR, Sherman LS, Sumner DY, Summons RE (2009) Late Archean molecular fossils from the Transvaal Supergroup record the antiquity of microbial diversity and aerobiosis. *Precambrian Res* 169(1–4):28–47.
71. Stüeken EE, Catling DC, Buick R (2012) Contributions to late Archean sulphur cycling by life on land. *Nat Geosci* 5(10):722–725.
72. Schopf JW (1993) Microfossils of the Early Archean Apex chert: New evidence of the antiquity of life. *Science* 260(5108):640–646.
73. Brasier M, McLoughlin N, Green O, Wacey D (2006) A fresh look at the fossil evidence for early Archean cellular life. *Philos Trans R Soc Lond B Biol Sci* 361(1470):887–902.
74. Bilofsky HS, Burks C (1988) The GenBank genetic sequence data bank. *Nucleic Acids Res* 16(5):1861–1863.
75. Edgar RC (2004) MUSCLE: multiple sequence alignment with high accuracy and high throughput. *Nucleic Acids Res* 32(5):1792–1797.
76. Akaike H (1974) New look at statistical-model identification. *IEEE Trans Automat Contr AC19(6):716–723.*
77. Hurvich CM, Tsai CL (1989) Regression and time-series model selection in small samples. *Biometrika* 76(2):297–307.
78. Posada D (2008) jModelTest: Phylogenetic model averaging. *Mol Biol Evol* 25(7):1253–1256.
79. Lanave C, Preparata G, Saccone C, Serio G (1984) A new method for calculating evolutionary substitution rates. *J Mol Evol* 20(1):86–93.
80. Drummond AJ, Rambaut A (2007) BEAST: Bayesian evolutionary analysis by sampling trees. *BMC Evol Biol* 7:214.
81. Rippka R, Waterbury J, Cohen-Bazire G (1974) Cyanobacterium which lacks thylakoids. *Arch Microbiol* 100(1):419–436.
82. Nakamura Y, et al. (2003) Complete genome structure of *Gloeobacter violaceus* PCC 7421, a cyanobacterium that lacks thylakoids. *DNA Res* 10(4):137–145.
83. Ferris MJ, Ruff-Roberts AL, Kopczynski ED, Bateson MM, Ward DM (1996) Enrichment culture and microscopy reveal diverse thermophilic *Synechococcus* populations in a single hot spring microbial mat habitat. *Appl Environ Microbiol* 62(3):1045–1050.
84. Miller M, et al. (2009) The CIPRES portals. CIPRES. Available at: www.phylo.org/submit-sections/portal. Accessed February 2012.
85. Sukumaran J, Holder MT (2010) DendroPy: A Python library for phylogenetic computing. *Bioinformatics* 26(12):1569–1571.
86. Golubic S, Sergeev VN, Knoll AH (1995) Mesoproterozoic Archaeoellipsoids: Akinetes of heterocystous cyanobacteria. *Lethaia* 28:285–298.
87. Alfaro ME, et al. (2009) Nine exceptional radiations plus high turnover explain species diversity in jawed vertebrates. *Proc Natl Acad Sci USA* 106(32):13410–13414.

Supporting Information

Schirrmeister et al. 10.1073/pnas.1209927110

SI Text

Taxon Sampling. Strain “G40” (deposited in GenBank) is a yet-uncharacterized, terminally differentiated, multicellular isolate from the North Sea. Its closest relative based on 16S rRNA sequences is *Nodularia*. Strain G40 was isolated from ponds at the shore of northwestern Ameland, The Netherlands. The strain was then cultivated in ASN III seawater medium and kept at 15 °C in an environmental chamber at a constant day/night cycle of 6 h darkness and 18 h light.

Phylogenetic Analyses. Phylogenetic relationships were estimated using MrBayes v.3.1.2 (1). We used two Markov chain Monte Carlo runs, each calculating six Metropolis-coupled chains for 100 million generations sampling every 2,000th generation. Default priors were adequate and left unchanged, but the temperature parameter was adjusted to 0.1 to ensure proper mixing. Convergence between runs was achieved, as the potential scale reduction factor had approached 1.00 and average SDs of split frequencies was <0.01. Mixing and convergence of all parameters was further assessed using the software Tracer v1.5 (2). We combined runs after discarding the first 25% of samples as a conservative burn-in, including only samples from the stationary phase. Effective sample sizes were large (>3,000) for the likelihood samples and all estimated parameters, supporting a well-mixed analysis. The Bayesian 50% majority-rule consensus tree is shown in Fig. S1.

1. Ronquist F, Huelsenbeck JP (2003) MrBayes 3: Bayesian phylogenetic inference under mixed models. *Bioinformatics* 19(12):1572–1574.
2. Rambaut A, Drummond AJ (2007) Tracer v1.4. Available at <http://tree.bio.ed.ac.uk/software/tracer>. Accessed January 2012.
3. Altschul SF, et al. (1997) Gapped BLAST and PSI-BLAST: A new generation of protein database search programs. *Nucleic Acids Res* 25(17):3389–3402.
4. Cuzman OA, et al. (2010) Biodiversity of phototrophic biofilms dwelling on monumental fountains. *Microb Ecol* 60(1):81–95.
5. Turner S, Prys KM, Miao VPW, Palmer JD (1999) Investigating deep phylogenetic relationships among cyanobacteria and plastids by small subunit rRNA sequence analysis. *J Eukaryot Microbiol* 46(4):327–338.
6. Nakamura Y, et al. (2002) Complete genome structure of the thermophilic cyanobacterium *Thermosynechococcus elongatus* BP-1. *DNA Res* 9(4):123–130.
7. Lyra C, et al. (2001) Molecular characterization of planktic cyanobacteria of *Anabaena*, *Aphanizomenon*, *Microcystis* and *Planktothrix* genera. *Int J Syst Evol Microbiol* 51(Pt 2): 513–526.
8. Casamatta DA, Johansen JR, Vis ML, Broadwater ST (2005) Molecular and morphological characterisation of ten polar and near-polar strains with the Oscillatoriaceae (cyanobacteria). *J Phycol* 41:421–438.
9. Ishida T, Watanabe MM, Sugiyama J, Yokota A (2001) Evidence for polyphyletic origin of the members of the orders of Oscillatoriaceae and Pleurocapsales as determined by 16S rRNA analysis. *FEMS Microbiol Lett* 201(1):79–82.
10. Ishida T, Yokota A, Sugiyama J (1997) Phylogenetic relationships of filamentous cyanobacterial taxa inferred from 16S rRNA sequence divergence. *J Gen Appl Microbiol* 43(4):237–241.
11. Janssen PJ, et al. (2010) Genome sequence of the edible cyanobacterium *Arthrosphaera* sp. PCC 8005. *J Bacteriol* 192(9):2465–2466.
12. Tomitani A, Knoll AH, Cavanaugh CM, Ohno T (2006) The evolutionary diversification of cyanobacteria: Molecular-phylogenetic and paleontological perspectives. *Proc Natl Acad Sci USA* 103(14):5442–5447.
13. Fuller NJ, et al. (2003) Clade-specific 16S ribosomal DNA oligonucleotides reveal the predominance of a single marine *Synechococcus* clade throughout a stratified water column in the Red Sea. *Appl Environ Microbiol* 69(5):2430–2443.
14. Urbach E, Scanlan DJ, Distel DL, Waterbury JB, Chisholm SW (1998) Rapid diversification of marine picophytoplankton with dissimilar light-harvesting structures inferred from sequences of *Prochlorococcus* and *Synechococcus* (Cyanobacteria). *J Mol Evol* 46(2): 188–201.
15. Moore LR, Rocap G, Chisholm SW (1998) Physiology and molecular phylogeny of coexisting *Prochlorococcus* ecotypes. *Nature* 393(6684):464–467.
16. Ernst A, Becker S, Wollenzien UIA, Postius C (2003) Ecosystem-dependent adaptive radiations of picocyanobacteria inferred from 16S rRNA and ITS-1 sequence analysis. *Microbiology* 149(Pt 1):217–228.
17. Sugita C, et al. (2007) Complete nucleotide sequence of the freshwater unicellular cyanobacterium *Synechococcus elongatus* PCC 6301 chromosome: Gene content and organization. *Photosynth Res* 93(1–3):55–67.
18. van Haren EJ, et al. (1999) Changes in bacterial and eukaryotic community structure after mass lysis of filamentous cyanobacteria associated with viruses. *Appl Environ Microbiol* 65(2):795–801.
19. Siivonen LM, et al. (2007) Strains of the cyanobacterial genera *Calothrix* and *Rivularia* isolated from the Baltic Sea display cryptic diversity and are distantly related to *Gloetrichia* and *Tolyphothrix*. *FEMS Microbiol Ecol* 61(1):74–84.
20. Boone DR, Castenholz RW (2001) *Bergey's Manual of Systematic Bacteriology: The Archaea and the Deeply Branching and Phototropic Bacteria: Cyanobacteria*, ed Garrity GM (Springer, New York).
21. Wilmette A, Auwera G, DeWachter R (1992) Structure of the 16S ribosomal RNA of the thermophilic cyanobacterium *Chlorogloeopsis* HTF ('*Mastigocladus laminosus* HTF') strain PCC75 18, and phylogenetic analysis. *FEBS Lett* 317(1–2):96–100.
22. Pointing SB, Warren-Rhodes KA, Lacap DC, Rhodes KL, McKay CP (2007) Hypolithic community shifts occur as a result of liquid water availability along environmental gradients in China's hot and cold hyperarid deserts. *Environ Microbiol* 9(2):414–424.
23. Nguyen VLA, Tanabe Y, Matsuura H, Kaya K, Watanabe MM (2012) Morphological, biochemical and phylogenetic assessments of water-bloom-forming tropical morphospecies of *Microcystis* (Chroococcales, Cyanobacteria). *Phycological Res* 60:208–222.
24. Winder B, Stal LJ, Mur LR (1990) *Crinalium epipappum* sp. nov.: A filamentous cyanobacterium with trichomes composed of elliptical cells and containing poly-β-(1,4) glucan (cellulose). *Microbiology* 136(8):1645–1653.
25. Turner S, Huang TC, Chaw SM (2001) Molecular phylogeny of nitrogen fixing unicellular cyanobacteria. *Bot Bull Acad Sin* 42:181–186.
26. Nübel U, Garcia-Pichel F, Muyzer G (1997) PCR primers to amplify 16S rRNA genes from cyanobacteria. *Appl Environ Microbiol* 63(8):3327–3332.
27. Fewer D, Friedl T, Buelel B (2002) Chroococcidiopsis and heterocyst-differentiating cyanobacteria are each others closest living relatives. *Mol Phyl Evol* 23(1):82–90.
28. Nelissen B, Van de Peer Y, Wilmette A, De Wachter R (1995) An early origin of plastids within the cyanobacterial divergence is suggested by evolutionary trees based on complete 16S rRNA sequences. *Mol Biol Evol* 12(6):1166–1173.
29. Ionescu D, Hindiyeh MY, Malkawi HI, Oren A (2010) Biogeography of thermophilic cyanobacteria: Insights from the Zerka Ma'in hot springs (Jordan). *FEMS Microbiol Ecol* 72(1):103–113.
30. Oren A, Ionescu D, Hindiyeh M, Malkawi H (2009) Morphological, phylogenetic and physiological diversity of cyanobacteria in the hot springs of Zerka Ma'in, Jordan. *BioRisk* 3(Special Issue):69–82.
31. Lehtimäki J, et al. (2000) Characterization of *Nodularia* strains, cyanobacteria from brackish waters, by genotypic and phenotypic methods. *Int J Syst Evol Microbiol* 50(Pt 3):1043–1053.

Morphotype Assessment. To ensure morphological character states (unicellular/multicellular) were assigned correctly for each cyanobacterial taxon used in this study, we carefully examined original publications describing the morphology of each strain. Furthermore, we conducted BLAST analyses (3) for each sequence to reassure its identity. In cases where the publication containing the original description of a strain was not available, we examined the closest 16S rRNA relative (identified from the BLAST results, ≥95% maximum identity) for which a publication was available. For each strain, additional information found in the literature (4–44) is listed in Table S5. Furthermore, a close BLAST result is given for each taxon including percentage of its maximum identity (Table S5).

Shifts in Diversification Rates. The function MEDUSA from the geiger 1.3-1 package in R (45) uses maximum likelihood to estimate a birth-death model of diversification that includes the optimal number of rate shifts, but penalizes for excess parameters based on Akaike Information Criterion (AIC) scores. Phylogenetic positions of unsampled species and strains in the cyanobacterial phylum were estimated with help of a phylogenetic tree of 1,220 taxa compiled in a previous study (46). Subsequently, numbers of unsampled species and strains were assigned to taxa sampled for the dating analyses of this study (Table S3). Inferences based on maximum clade credibility trees gave qualitatively similar results.

32. Voss JD, Mills DK, Myers JL, Remily ER, Richardson LL (2007) Black band disease microbial community variation on corals in three regions of the wider Caribbean. *Microb Ecol* 54(4):730–739.
33. Nakamura Y, et al. (2003) Complete genome structure of *Gloeobacter violaceus* PCC 7421, a cyanobacterium that lacks thylakoids. *DNA Res* 10(4):137–145.
34. Micheletti E, et al. (2008) Sheathless mutant of Cyanobacterium *Gloeothecae* sp. strain PCC 6909 with increased capacity to remove copper ions from aqueous solutions. *Appl Environ Microbiol* 74(9):2797–2804.
35. Nübel U, Garcia-Pichel F, Muyzer G (2000) The halotolerance and phylogeny of cyanobacteria with tightly coiled trichomes (*Spirulina Turpin*) and the description of *Halospirulina tapetica* gen. nov., sp. nov. *Int J Syst Evol Microbiol* 50(Pt 3):1265–1277.
36. Taton A, et al. (2006) Polyphasic study of antarctic cyanobacterial strains. *J Phycol* 42(6):1257–1270.
37. Pomati F, Sacchi S, Rossetti C, Giovannardi S (2000) The freshwater cyanobacterium *Planktothrix* sp. FP1: Molecular identification and detection of paralytic shellfish poisoning toxins. *J Phycol* 36(3):553–562.
38. Marin B, Nowack ECM, Glöckner G, Melkonian M (2007) The ancestor of the *Paulinella* chromatophore obtained a carboxysomal operon by horizontal gene transfer from a *Nitrococcus*-like γ -proteobacterium. *BMC Evol Biol* 7:85.
39. Ligon PJB, Meyer KG, Martin JA, Curtis SE (1991) Nucleotide sequence of a 16S rRNA gene from *Anabaena* sp. strain PCC 7120. *Nucleic Acids Res* 19(16):4553.
40. El-Shehawy R, Lugomela C, Ernst A, Bergman B (2003) Diurnal expression of hetR and diazocyte development in the filamentous non-heterocystous cyanobacterium *Trichodesmium erythraeum*. *Microbiology* 149(Pt 5):1139–1146.
41. Zwart G, et al. (2005) Molecular characterization of cyanobacterial diversity in a shallow eutrophic lake. *Environ Microbiol* 7(3):365–377.
42. Urbach E, Robertson DL, Chisholm SW (1992) Multiple evolutionary origins of prochlorophytes within the cyanobacterial radiation. *Nature* 355(6357):267–270.
43. Kaneko T, et al. (1996) Sequence analysis of the genome of the unicellular cyanobacterium *Synechocystis* sp. strain PCC6803. II. Sequence determination of the entire genome and assignment of potential protein-coding regions. *DNA Res* 3(3):109–136.
44. Gugger MF, Hoffmann L (2004) Polyphyly of true branching cyanobacteria (Stigonematales). *Int J Syst Evol Microbiol* 54(Pt 2):349–357.
45. Alfaro ME, et al. (2009) Nine exceptional radiations plus high turnover explain species diversity in jawed vertebrates. *Proc Natl Acad Sci USA* 106(32):13410–13414.
46. Schirrmeyer BE, Antonelli A, Bagheri HC (2011) The origin of multicellularity in cyanobacteria. *BMC Evol Biol* 11:45.

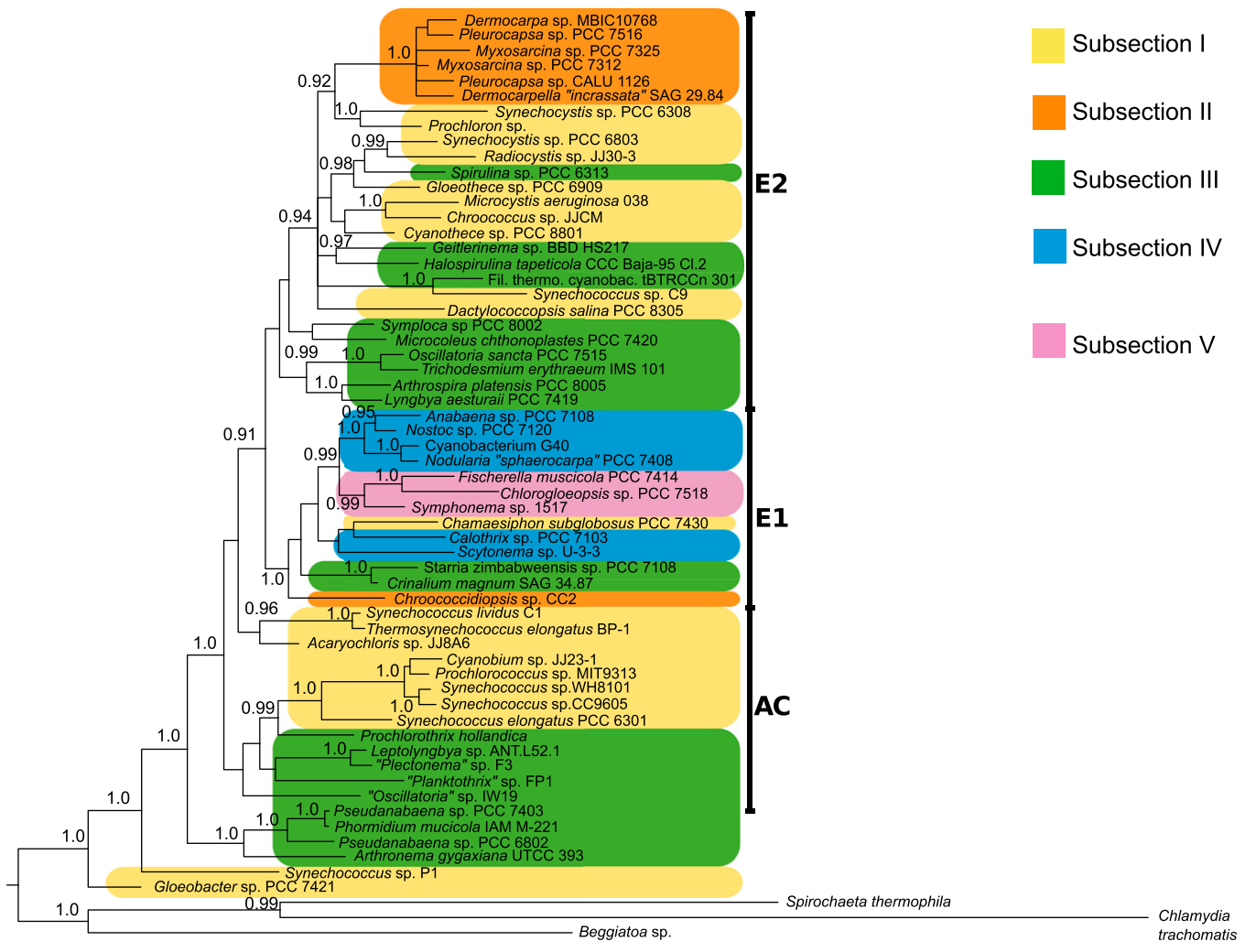


Fig. S1. Bayesian 50% majority-rule consensus phylogram, based on MrBayes analysis. Posterior probabilities shown at nodes when >0.90. Unicellular cyanobacteria belonging to sections I and II are marked by yellow and orange, whereas multicellular cyanobacteria from sections III, IV, and V are marked by green, blue, and purple, respectively. *Gloeobacter violaceus* groups closest to the eubacterial outgroup.

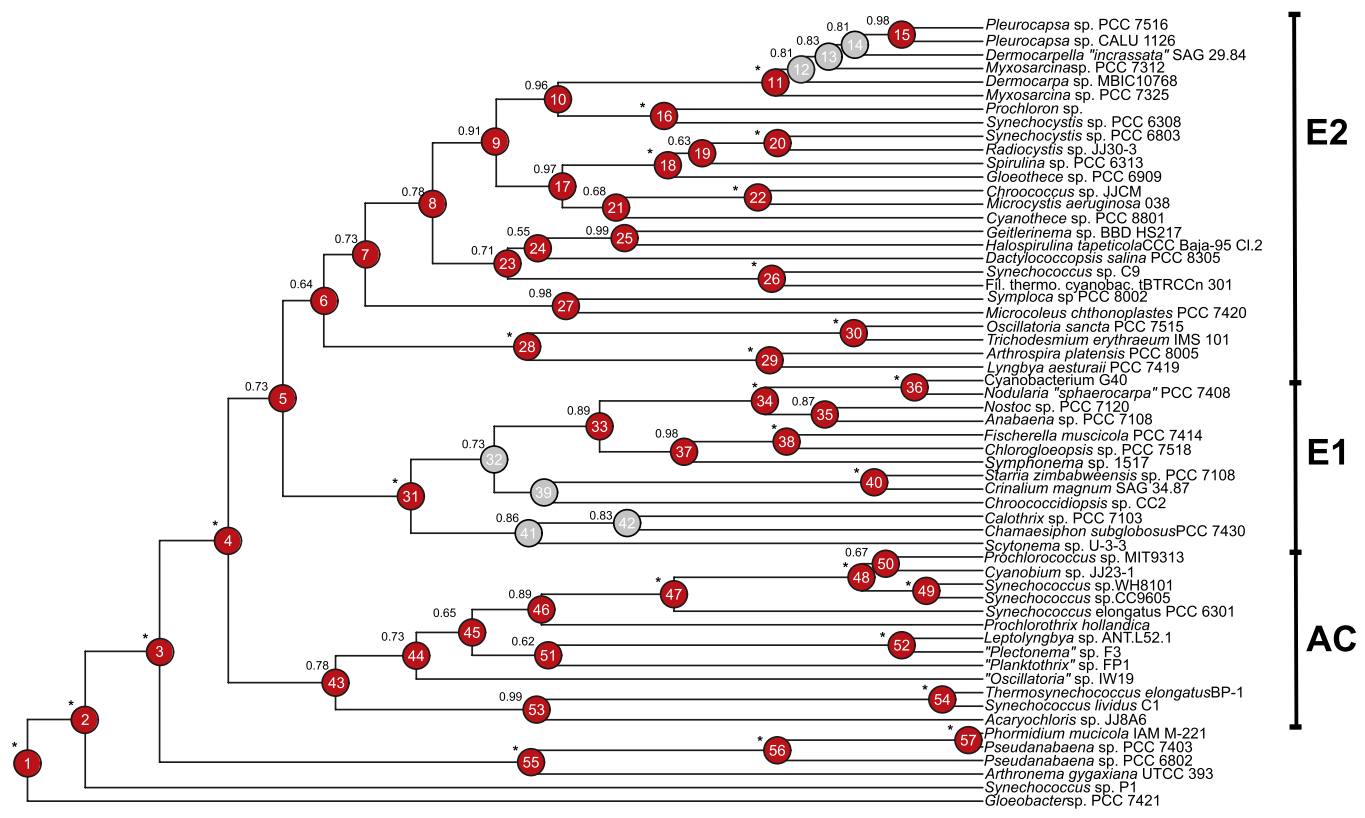


Fig. S2. Bayesian consensus tree of BEAST analysis 7. Posterior probabilities and node numbers are presented at nodes. Gray nodes were not recovered by all analyses.

Rate shift - species (ucln)

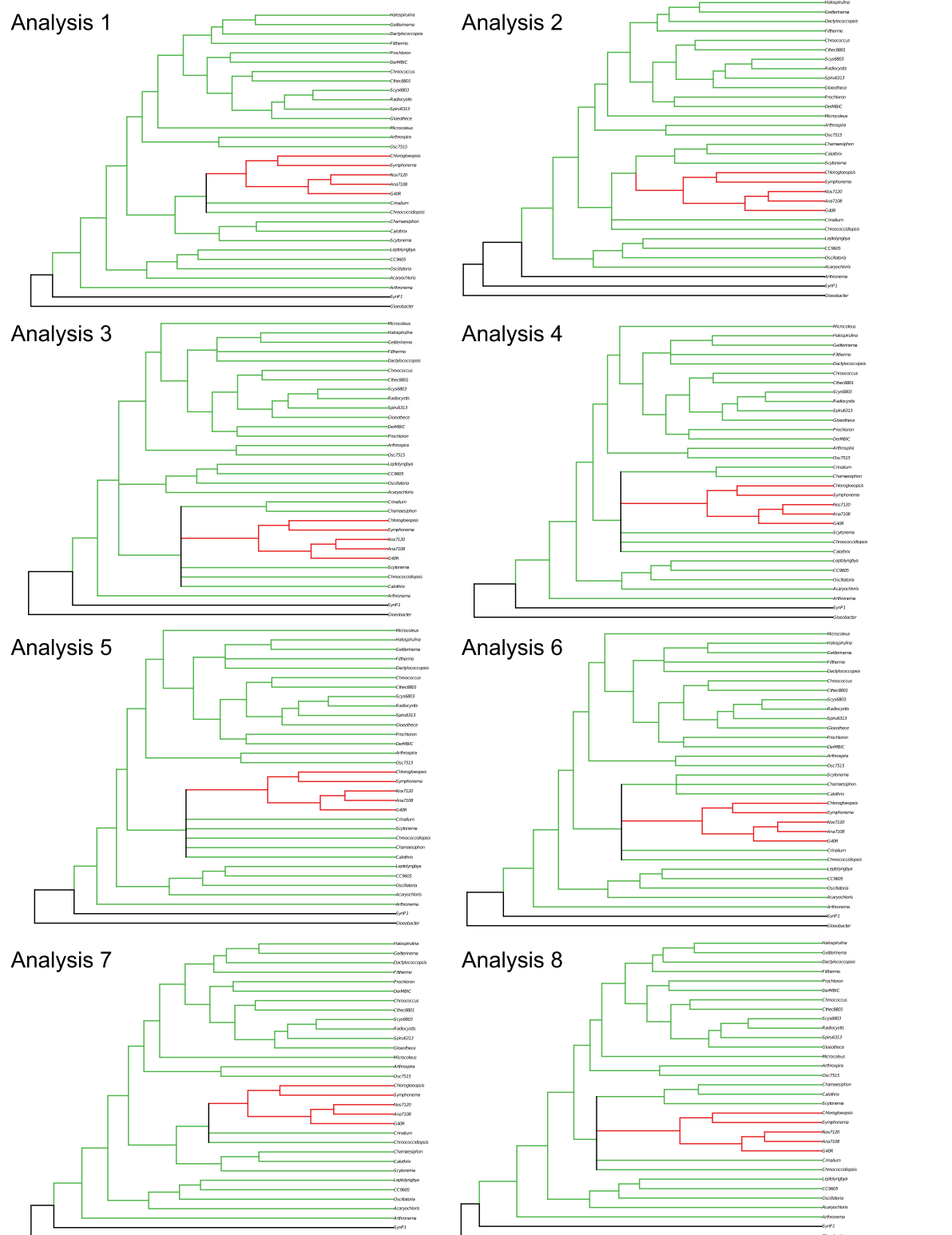


Fig. S3. Clade-specific diversification rates using species numbers (uncorrelated lognormal, UCLN). Results of MEDUSA analyses indicating diversification rate shifts for the different consensus trees from the Bayesian analyses assuming uncorrelated lognormally distributed evolutionary rates.

Rate shift - strains (ucln)

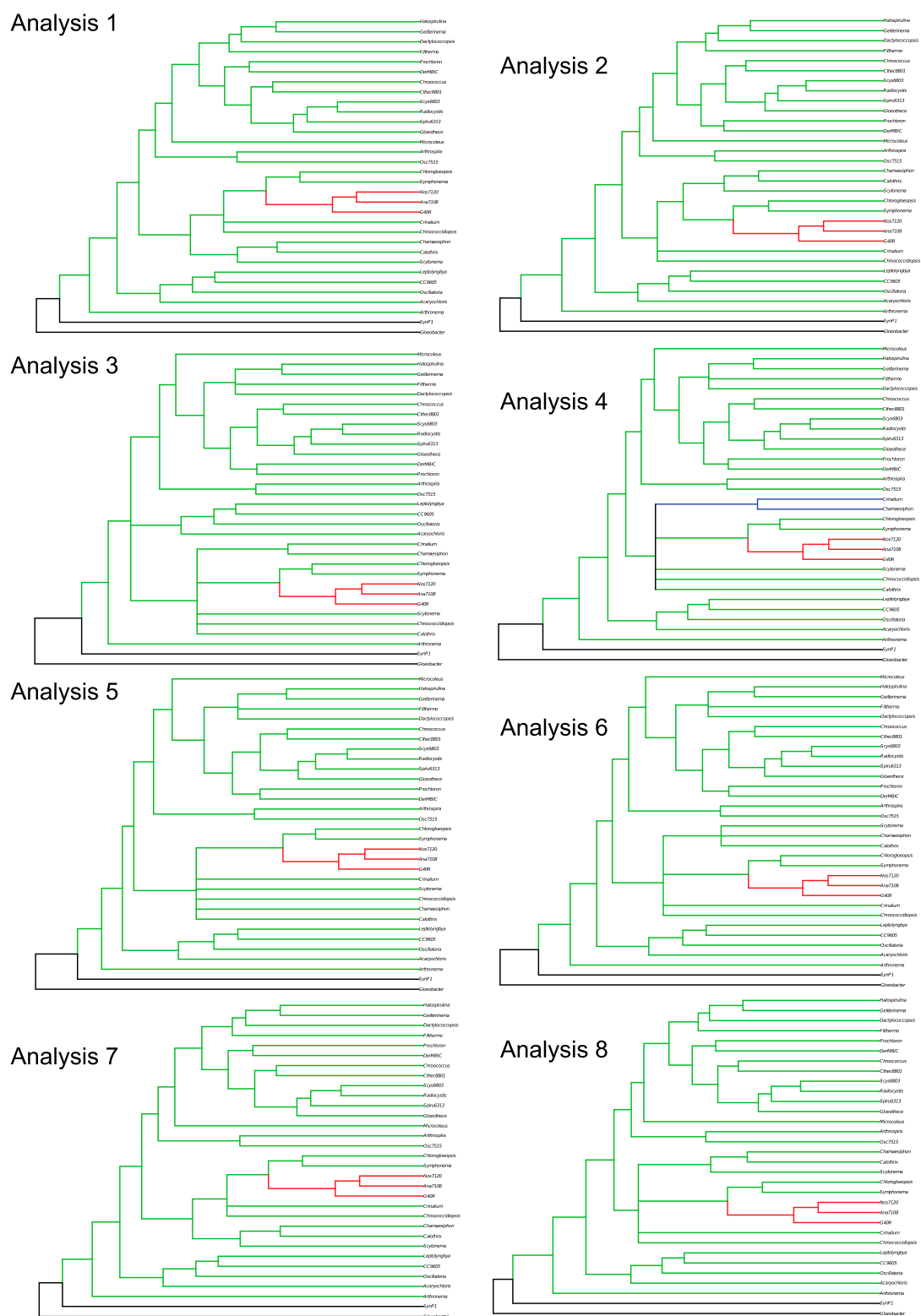


Fig. S4. Clade-specific diversification rates using strain numbers (UCLN). Results of MEDUSA analyses indicating diversification rate shifts for the different consensus trees from the Bayesian analyses assuming UCLN distributed evolutionary rates.

Rate shifts - species (uced)

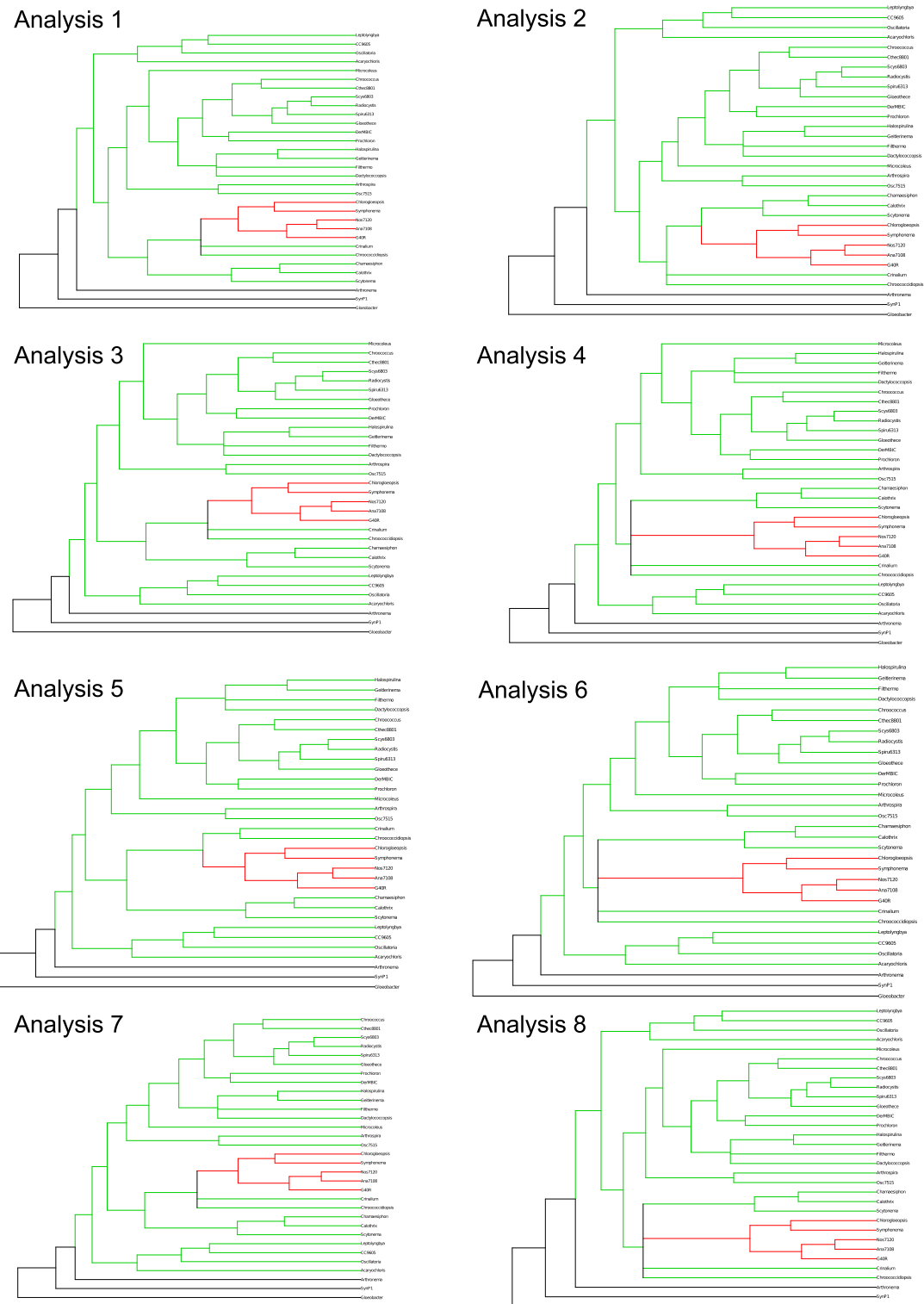


Fig. S5. Clade-specific diversification rates using species numbers (uncorrelated exponentially distributed, UCED). Results of MEDUSA analyses indicating diversification rate shifts for the different consensus trees from the Bayesian analyses assuming UCED evolutionary rates.

Rate shifts - strains (uced)

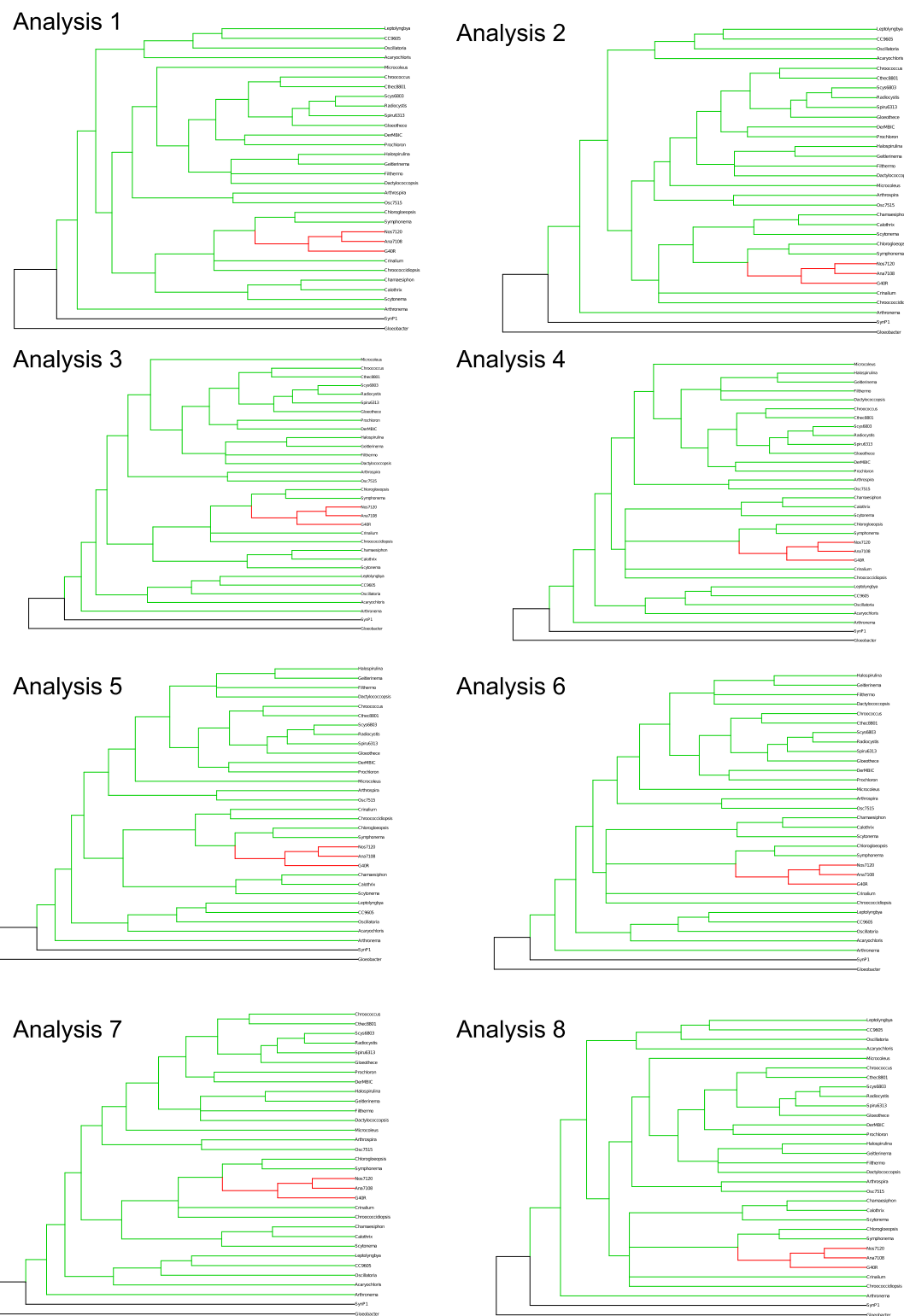


Fig. S6. Clade-specific diversification rates using strain numbers (UCED). Results of MEDUSA analyses indicating diversification rate shifts for the different consensus trees from the Bayesian analyses assuming UCED evolutionary rates.

Table S1. Divergence times for five important nodes estimated using a relaxed clock with UCED evolutionary rates

Analysis	1	2	3	4	5	6	7	8
Model assumptions and calibration points	—	—	Yes	Yes	Yes	Yes	—	—
Outgr.	—	—	Exp (2.45;2.816)	Exp (2.45;2.816)*	Exp (2.45;2.816)*	Exp (2.45;2.816)*	—	*
Root	—	—	LN(2.1;2.27,0.5)	LN(2.1;2.27,0.5)	LN(2.1;2.27,0.5)	LN(2.1;2.27,0.5)	LN(2.1;2.27,0.5)	*
Node 3	LN(2.1;2.27,0.5)	LN(2.1;2.58,0.8)	LN(2.1;2.58,0.8)	LN(2.1;2.58,0.8)	LN(2.1;2.58,0.8)	LN(2.1;2.58,0.8)	LN(2.1;2.58,0.8)	*
Node 31 or 32	LN(2.1;2.13,1)	LN(2.1;2.13,1)	LN(2.1;2.13,1)	LN(2.1;2.13,1)	LN(2.1;2.13,1)	LN(2.1;2.13,1)	LN(2.1;2.13,1)	LN(2.1;2.13,1)
Results for discussed nodes (UCED) (\tilde{m}) (HPD) for all	—	—	—	—	—	—	—	—
Node 1	2.95 (2.39–3.99)	3.72 (2.62–5.40)	2.81 (2.41–3.36)	3.17 (2.58–4.0)	2.82 (2.45–3.30)	3.06 (2.60–5.60)	2.93 (2.45–3.60)	3.33 (2.78–3.80)
Node 3	2.44 (2.21–2.80)	2.95 (2.31–3.97)	2.37 (2.20–2.60)	2.6 (2.25–3.13)	2.39 (2.20–2.65)	2.55 (2.24–2.93)	2.44 (2.23–2.8)	2.75 (2.32–3.25)
Node 6	2.00 (1.52–2.31)	2.21 (1.65–2.91)	1.97 (1.48–2.27)	2.04 (1.49–2.50)	1.96 (1.43–2.30)	2.02 (1.45–2.44)	2 (1.56–2.25)	2.11 (1.63–2.58)
Node 31	1.82 (1.12–2.28)	2.16 (1.43–2.65)	1.76 (1.07–2.24)	2.12 (1.24–2.42)	1.85 (1.11–2.27)	2.12 (1.2–2.4)	1.85 (2–2.29)	2.13 (1.27–2.44)
Node 43	1.91 (1.15–2.43)	2.2 (1.31–3.11)	1.8 (1.5–2.29)	1.94 (1.17–2.6)	1.81 (1.11–2.30)	1.9 (1.17–2.47)	1.91 (1.24–2.4)	2.07 (1.32–2.73)

Exp, exponential distribution (offset,mean); LN, lognormal distribution (offset,mean, SD); —, not applicable.
*Truncated at 3.8 Bya.

Table S2. Estimated Ages of nodes found in the Bayesian consensus trees (reconstructed with UCLN rates) for each analyses. Nd - node number

Node	\bar{m}	Lo	Up	1		2		3		4		5		6		7		8							
				\bar{m}	Lo	\bar{m}	Lo	Up																	
1	2.95	2.5	3.6	3.67	2.79	4.74	2.99	2.57	3.55	2.74	4.15	2.87	2.53	3.30	3.06	2.66	3.53	2.95	2.53	3.39	2.87	3.80			
2	2.77	2.42	3.29	3.47	2.67	4.40	2.63	2.35	2.98	2.96	2.49	3.61	2.56	2.33	2.84	2.75	2.44	3.14	2.77	2.43	3.28	3.22	3.72		
3	2.54	2.28	2.98	3.08	2.42	3.84	2.42	2.21	2.73	2.65	2.28	3.18	2.38	2.20	2.62	2.49	2.26	2.81	2.54	2.29	2.97	2.86	3.34		
4	2.33	2.14	2.7	2.76	2.21	3.39	2.24	2.12	2.47	2.40	2.14	2.84	2.22	2.12	2.39	2.28	2.13	2.54	2.33	2.14	2.68	2.58	3.01		
5	2.16	2.1	2.45	2.50	2.10	3.02	2.24	2.24	2.10	2.10	2.60	2.14	2.10	2.25	2.16	2.10	2.37	2.16	2.10	2.44	2.33	2.10	2.70		
6	2.04	1.77	2.35	2.33	1.89	2.87	2.02	1.72	2.28	2.10	1.78	2.54	1.99	1.67	2.22	2.02	1.70	2.32	2.04	1.79	2.35	2.18	1.86	2.60	
7	1.91	1.62	2.25	2.21	1.74	2.78	1.89	1.57	2.17	1.99	1.63	2.41	1.85	1.53	2.13	1.89	1.56	2.21	1.91	1.62	2.24	2.07	1.71	2.50	
8	1.7	1.41	2.03	1.98	1.53	2.53	1.67	1.35	1.99	1.77	1.41	2.20	1.61	1.29	1.92	1.65	1.31	1.99	1.70	1.41	2.03	1.85	1.51	2.26	
9	1.5	1.2	1.82	1.75	1.32	2.26	1.46	1.14	1.79	1.56	1.19	1.97	1.40	1.08	1.72	1.43	1.09	1.76	1.50	1.20	1.82	1.64	1.29	2.03	
10	1.31	1	1.66	1.53	1.09	2.02	1.26	0.91	1.62	1.35	0.95	1.76	1.19	0.85	1.54	1.22	0.87	1.59	1.31	0.99	1.65	1.44	1.08	1.83	
11	0.64	0.43	0.88	0.75	0.48	1.07	0.58	0.38	0.84	0.63	0.39	0.91	0.56	0.34	0.81	0.57	0.36	0.83	0.64	0.43	0.88	0.70	0.47	0.98	
12	0.56	0.37	0.78	0.66	0.42	0.94	—	—	—	—	—	—	—	—	—	—	—	—	—	—	—	—	—	0.86	
13	0.48	0.31	0.67	0.56	0.34	0.81	—	—	—	—	—	—	—	—	—	—	—	—	—	—	—	—	—	0.74	
14	0.39	0.24	0.58	0.46	0.27	0.70	—	—	—	—	—	—	—	—	—	—	—	—	—	—	—	—	—	0.64	
15	0.25	0.13	0.41	0.29	0.15	0.49	0.26	0.12	0.45	0.28	0.12	0.48	0.24	0.10	0.43	0.25	0.11	0.44	0.25	0.13	0.40	0.27	0.14	0.44	
16	0.98	0.62	1.35	1.14	0.70	1.65	0.91	0.52	1.30	0.98	0.55	1.43	0.85	0.45	1.24	0.87	0.47	1.28	0.98	0.61	1.34	1.08	0.68	1.50	
17	1.3	0.99	1.62	1.51	1.10	1.99	1.25	0.93	1.58	1.34	0.98	1.74	1.19	0.87	1.52	1.22	0.89	1.56	1.29	0.99	1.61	1.42	1.08	1.80	
18	0.97	0.68	1.3	1.13	0.75	1.57	0.96	0.65	1.30	1.03	0.69	1.42	0.90	0.58	1.23	0.93	0.60	1.28	0.97	0.67	1.29	1.06	0.73	1.42	
19	0.87	0.58	1.18	1.01	0.64	1.42	0.83	0.52	1.15	0.89	0.57	1.27	0.77	0.47	1.09	0.80	0.49	1.13	0.86	0.58	1.18	0.95	0.62	1.29	
20	0.63	0.36	0.93	0.74	0.41	1.11	0.58	0.31	0.90	0.63	0.33	0.97	0.54	0.26	0.84	0.55	0.27	0.86	0.63	0.36	0.93	0.69	0.40	1.02	
21	1.13	0.78	1.49	1.32	0.86	1.80	1.05	0.68	1.41	1.12	0.72	1.55	0.99	0.62	1.36	1.01	0.65	1.39	1.13	0.78	1.49	1.24	0.86	1.64	
22	0.69	0.39	1.04	0.81	0.42	1.26	0.62	0.32	0.98	0.66	0.31	1.04	0.57	0.26	0.92	0.59	0.28	0.95	0.69	0.37	1.04	0.76	0.42	1.15	
23	1.47	1.15	1.82	1.70	1.25	2.25	1.42	1.07	1.77	1.52	1.11	1.94	1.36	0.97	1.70	1.39	1.01	1.76	1.47	1.14	1.81	1.59	1.21	2.00	
24	1.37	0.99	1.75	1.58	1.07	2.12	—	—	—	—	—	—	—	—	—	—	—	—	—	—	—	—	—	1.92	
25	1.11	0.68	1.52	0.75	0.51	1.85	1.06	0.60	1.51	1.13	0.62	1.63	0.99	0.53	1.46	1.01	0.54	1.52	1.10	0.67	1.51	1.20	0.73	1.68	
26	0.65	0.36	1.01	0.76	0.40	1.23	0.63	0.30	1.01	0.68	0.32	1.13	0.58	0.27	0.97	0.60	0.28	1.00	0.65	0.37	0.98	0.71	0.39	1.09	
27	1.29	0.66	1.82	1.47	0.75	2.18	1.16	0.53	1.75	1.24	0.56	1.89	1.12	0.50	1.74	1.17	0.49	1.80	1.28	0.67	1.82	1.39	0.73	2.01	
28	1.41	0.91	1.89	1.61	1.01	2.27	1.26	0.77	1.80	1.36	0.79	1.94	1.23	0.72	1.81	1.29	0.75	1.86	1.41	0.92	1.89	1.52	0.98	2.07	
29	0.66	0.3	1.11	0.76	0.34	1.06	0.59	0.24	1.06	0.64	0.26	1.13	0.57	0.22	1.06	0.59	0.23	1.09	0.66	0.31	1.12	0.72	0.33	1.20	
30	0.4	0.18	0.7	0.46	0.19	0.81	0.36	0.14	0.67	0.39	0.15	0.74	0.35	0.13	0.68	0.36	0.12	0.71	0.40	0.18	0.70	0.43	0.19	0.76	
31	1.77	1.4	2.24	2.16	1.53	2.56	1.72	1.34	2.20	1.98	1.39	2.34	1.67	1.28	2.17	1.75	1.30	2.23	1.77	1.41	2.25	2.12	1.50	2.41	
32	1.51	1.18	1.81	1.92	1.59	2.18	—	—	—	—	—	—	—	—	—	—	—	—	—	—	—	—	—	—	—
33	1.18	0.85	1.58	1.44	0.99	1.85	1.08	0.76	1.44	1.17	0.79	1.62	1.02	0.70	1.39	1.06	0.72	1.47	1.19	0.87	1.60	1.33	0.94	1.75	
34	0.67	0.41	1	0.81	0.47	1.21	0.64	0.36	0.95	0.69	0.39	1.07	0.60	0.33	0.92	0.63	0.35	0.97	0.68	0.40	1.00	0.75	0.44	1.12	
35	0.49	0.24	0.79	0.57	0.27	0.95	0.43	0.19	0.74	0.47	0.21	0.82	0.40	0.16	0.71	0.42	0.17	0.74	0.49	0.24	0.80	0.54	0.26	0.88	
36	0.21	0.09	0.38	0.25	0.11	0.47	0.20	0.07	0.39	0.22	0.08	0.43	0.19	0.06	0.37	0.20	0.06	0.40	0.21	0.09	0.38	0.23	0.09	0.43	
37	0.92	0.62	1.27	1.10	0.72	1.51	0.82	0.52	1.16	0.90	0.55	1.28	0.77	0.47	1.12	0.80	0.50	1.17	0.93	0.62	1.27	1.03	0.68	1.42	
38	0.61	0.35	0.9	0.72	0.41	1.07	0.53	0.28	0.82	0.57	0.30	0.90	0.49	0.25	0.79	0.51	0.26	0.82	0.61	0.36	0.91	0.67	0.39	1.00	
39	0.34	0.15	0.6	0.40	0.17	0.72	0.29	0.12	0.56	0.32	0.12	0.62	0.27	0.09	0.54	0.29	0.10	0.58	0.34	0.15	0.60	0.37	0.16	0.67	
40	1.4	0.98	1.8	1.53	1.09	1.93	—	—	—	—	—	—	—	—	—	—	—	—	—	—	—	—	—	1.87	
41	1.1	0.66	1.56	1.20	0.72	1.65	—	—	—	—	—	—	—	—	—	—	—	—	—	—	—	—	—	1.62	
42	2	1.56	2.43	2.35	1.73	3.03	1.85	1.46	2.25	1.97	1.48	2.50	1.80	1.38	2.19	1.54	1.12	2.04	1.75	2.30	2.00	1.57	2.18	2.72	
43	1.75	1.34	2.18	2.05	1.47	2.72	1.59	1.19	1.98	1.70	1.23	2.22	1.54	1.07	2.00	1.36	0.98	1.74	1.40	1.02	1.84	1.58	1.20	1.71	
44	1.58	1.19	1.98	1.85	1.32	2.47	1.42	1.05	1.79	1.51	1.07	2.00	1.36	0.98	1.74	1.40	1.02	1.84	1.58	1.20	1.97	1.71	1.30	2.21	

Table S2. Cont.

Node	1		2		3		4		5		6		7		8									
	\bar{m}	Lo	Up																					
46	1.36	0.99	1.76	1.60	1.09	2.16	0.84	1.57	1.28	0.87	1.75	1.13	0.78	1.51	1.17	0.79	1.58	1.37	0.99	1.77	1.50	1.07	1.97	
47	0.95	0.65	1.31	1.12	0.72	1.60	0.85	0.55	1.19	0.91	0.57	1.31	0.79	0.50	1.15	0.82	0.50	1.18	0.96	0.64	1.31	1.05	0.70	1.46
48	0.37	0.22	0.58	0.44	0.26	0.68	0.34	0.19	0.52	0.36	0.20	0.57	0.32	0.17	0.50	0.33	0.18	0.54	0.38	0.23	0.57	0.41	0.24	0.62
49	0.17	0.07	0.31	0.20	0.08	0.37	0.15	0.06	0.28	0.17	0.06	0.31	0.14	0.05	0.27	0.15	0.05	0.29	0.17	0.07	0.31	0.19	0.08	0.34
50	0.3	0.16	0.47	0.35	0.18	0.57	0.26	0.12	0.43	0.28	0.14	0.47	0.24	0.11	0.41	0.25	0.11	0.43	0.30	0.16	0.47	0.33	0.17	0.51
51	1.34	0.89	1.78	1.57	1.00	2.20	1.19	0.76	1.61	1.27	0.78	1.78	1.12	0.69	1.54	1.16	0.70	1.62	1.34	0.89	1.77	1.46	0.97	1.97
52	0.25	0.1	0.47	0.29	0.11	0.55	0.23	0.08	0.46	0.25	0.09	0.50	0.22	0.07	0.46	0.23	0.08	0.48	0.25	0.10	0.47	0.27	0.11	0.51
53	1.38	0.71	1.99	1.65	0.83	2.48	1.23	0.60	1.83	1.33	0.62	2.02	1.16	0.51	1.77	1.20	0.55	1.87	1.39	0.73	2.02	1.52	0.80	2.26
54	0.13	0.04	0.25	0.15	0.05	0.30	0.12	0.04	0.26	0.13	0.04	0.28	0.11	0.03	0.26	0.12	0.03	0.27	0.13	0.04	0.25	0.14	0.05	0.28
55	1.4	0.83	2.02	1.65	0.94	2.50	1.27	0.71	1.93	1.39	0.76	2.14	1.23	0.64	1.90	1.27	0.68	2.00	1.39	0.84	2.00	1.54	0.91	2.27
56	0.63	0.3	1.07	0.75	0.35	1.30	0.56	0.25	0.99	0.61	0.25	1.10	0.53	0.21	0.99	0.55	0.21	1.03	0.63	0.30	1.05	0.70	0.33	1.18
57	0.04	0.01	0.11	0.05	0.01	0.13	0.04	0.01	0.11	0.05	0.01	0.12	0.04	0.01	0.11	0.04	0.01	0.11	0.04	0.01	0.11	0.05	0.01	0.12

Lo, lower boundary of the 95% highest-posterior density; Up, upper boundary of the 95% highest-posterior density; —, not applicable.

Table S3. Names of taxa and corresponding numbers of species and strains to which they can be assigned in the cyanobacterial phylum

Taxa	No. species	No. strains	GenBank accession
<i>Acaryochloris</i> sp. JJ8A6* (4)	5	14	AM710387
<i>Synechococcus lividus</i> C1 [†] (5)			AF132772
<i>Thermosynechococcus elongatus</i> BP-1 [†] (6)			BA000039
<i>Anabaena</i> sp. PCC 7108 (7)	28	459	AJ133162
<i>Arthronema gygaxiana</i> UTCC 393 (8)	5	57	AF218370
<i>Pseudanabaena</i> sp. PCC 7304 [†] (9)			AB039019
<i>Pseudanabaena</i> sp. PCC 6802 [†] (9)			AB039016
" <i>Phormidium mucicola</i> " IAM M-221 [†] (10)			AB003165
<i>Arthrosphaera platenensis</i> PCC 8005 (11)	9	42	X70769
<i>Lyngbya aestuarii</i> PCC 7419 [†] (12)			AB075989
<i>Synechococcus</i> sp. CC9605 (13)	13	567	AY172802
<i>Synechococcus</i> sp. WH8101 [†] (14)			AF001480
<i>Prochlorococcus</i> sp. MIT 9313 [†] (15)			AF053399
<i>Cyanobium</i> sp. JJ23-1* [†] (16)			AM710371
<i>Synechococcus elongatus</i> PCC 6301 [†] (17)			AP008231
<i>Prochlorothrix hollandica</i> [†] (18)			AJ007907
<i>Calothrix</i> sp. PCC 7103 (19)	6	226	AM230700
<i>Chamaesiphon subglobosus</i> PCC 7430 (20)	1	2	AY170472
<i>Chlorogloeopsis</i> sp. PCC 7518 (21)	18	136	X68780
<i>Fischerella muscicola</i> PCC 7414 [†] (12)			AB075986
<i>Chroococcidiopsis</i> sp. CC2 (22)	3	51	DQ914864
<i>Chroococcus</i> sp. JJCM* (4)	10	325	AM710384
<i>Microcystis aeruginosa</i> strain 038* [†] (23)			DQ363254
<i>Crinalium magnum</i> SAG 34.87 [†] (24)	2	2	AB115965
<i>Starria zimbabweensis</i> SAG 74.90 [†] (20)			AB115962
<i>Cyanothece</i> sp. PCC 8801 (25)	4	22	AF296873
<i>Dactylococcopsis salina</i> PCC 8305 (26)	4	34	AJ000711
<i>Dermocarpa</i> sp. MBIC10768 (9)	8	41	AB058287
<i>Myxosarcina</i> sp. PCC 7312 [†] (27)			AJ344561
<i>Myxosarcina</i> sp. PCC 7325 [†] (27)			AJ344562
<i>Pleurocapsa</i> sp. CALU 1126* [†] (27)			DQ293994
<i>Pleurocapsa</i> sp. PCC 7516 [†] (28)			X78681
" <i>Dermocarrella incrassata</i> " SAG 29.84 [†] (27)			AJ344559
<i>Filamentous thermophilic cyanobacterium</i> tBTRCCn 301 (29, 30)	6	17	DQ471441
<i>Synechococcus</i> sp. C9 [†] (5)			AF132773
<i>Cyanobacterium</i> G40 (present study)	17	247	JX069960
" <i>Nodularia sphaerocarpa</i> " PCC 7804 [†] (31)			AJ133181
<i>Geitlerinema</i> sp. BBD HS217 (32)	8	97	EF110974
<i>Gloeobacter violaceus</i> PCC 7421 (33)	1	1	BA000045
<i>Gloeothece</i> sp. PCC 6909 (34)	3	13	HE975018
<i>Halospirulina tapetica</i> CCC Baja-95 Cl.2 (35)	2	6	NR_026510
<i>Leptolyngbya</i> sp. ANT.L52.1 (36)	6	332	AY493584
" <i>Planktothrix</i> " sp. FP1 [†] (37)			AF212922
" <i>Plectonema</i> " sp. F3 [†] (36)			AF091110
<i>Microcoleus chthonoplastes</i> PCC 7420 (38)	19	434	AM709630
<i>Symploca</i> sp. PCC 8002 [†] (9)			AB039021
<i>Nostoc</i> sp. PCC 7120 (39)	25	649	X59559
<i>Oscillatoria sancta</i> PCC 7515 (5)	30	129	AF132933
<i>Trichodesmium erythraeum</i> IMS 101 [†] (40)			AB075999
" <i>Oscillatoria</i> " sp. IW19 (41)	20	147	AJ133106
<i>Prochloron</i> sp. (42)	4	6	X63141
<i>Synechocystis</i> sp. PCC 6308 [†] (43)			AB039001
<i>Radio cystis</i> sp. JJ30-3* (44)	2	2	AM710389
<i>Synechocystis</i> sp. PCC 6803 (44)	4	51	NC_000911
<i>Scytonema</i> sp. U-3-3* (38)	4	45	AY069954
<i>Spirulina</i> sp. PCC 6313 (38)	6	29	X75045
<i>Sympytonema</i> sp. strain 1517 (45)	7	9	AJ544084
<i>Synechococcus</i> sp. P1 (5)	1	2	AF132774

Phylogenetic positions of taxa and the amount of species/strains they represent were estimated with help of a phylogenetic tree comprising 1,220 cyanobacterial taxa presented in the study by Schirrmeyer et al. (46).

*Citation for a close relative identified by BLAST search.

[†]Clades that have been pruned for the diversification rate analyses. Taxa with their names in quotes have likely been misidentified in the original publication considering their BLAST results.

Table S4. Estimated clade-specific diversification rates based on trees from eight phylogenetic analyses

Analysis	Species				Strains			
	Clade	r	ϵ	AICc	Clade	r	ϵ	AICc
UCLN distributed rates of evolution								
1	Root	0.17	4.73E-8		Root	0.28	7.79E-7	
	Node 3	1.63	9.07E-9	206.6	Node 3	2.39	0.8	357.7
	Node 33	1.37	0.93		Node 34	1.08	1.00	
2	Root	0.38	1.14E-8		Root	0.23	3.80E-7	371.2
	Node 4	1.43	2.31E-9	218.4	Node 3	1.91	0.83	
	Node 33	0.99	0.95		Node 34	0.78	1.00	
3	Root	0.17	4.67E-7		Root	0.28	1.07E-6	365.4
	Node 3	1.63	2.29E-7	212.6	Node 3	1.99	8.86E-001	
	Node 33	0.9	0.97		Node 34	1.06	1.00	
4	Root	0.15	5.03E-7		Root	0.25	1.79E-7	366.8
	Node 3	1.53	1.61E-7	216.4	Node 3	1.9	0.89	
	Node 33	0.7	0.97		Node 34	0.94	1.00	
5	Root	0.17	1.42E-7		Root	0.29	5.40E-7	368.1
	Node 3	1.68	3.22E-8	213.5	Node 3	1.88	0.9	
	Node 33	0.86	0.97		Node 34	1.06	1.00	
6	Root	0.16	1.24E-6		Root	0.27	3.49E-7	367.9
	Node 3	1.67	4.09E-7	212.4	Node 3	1.97	0.9	
	Node 33	0.81	0.97		Node 34	1.01	1.00	
7	Root	0.17	3.90E-10		Root	0.28	3.90E-7	357.8
	Node 3	1.63	2.45E-7	206.7	Node 3	2.39	0.8	
	Node 33	1.38	0.93		Node 34	1.07	1.00	
8	Root	0.15	4.42E-7		Root	0.24	7.89E-7	370.0
	Node 3	1.47	1.83E-7	216.3	Node 3	1.94	0.85	
	Node 33	0.74	0.97		Node 34	0.89	1.00	
UCED rates of evolution								
1	Root	0.48	3.66E-7		Root	0.28	9.96E-7	371.3
	Node 4	1.94	2.88E-2	211.9	Node 3	1.66	0.96	
	Node 33	1	0.97		Node 34	0.29	1.00	
2	Root	0.39	1.02E-8		Root	0.23	1.96E-8	377.7
	Node 4	1.67	7.07E-2	222.6	Node 3	1.36	0.96	
	Node 33	0.64	0.98		Node 34	0.18	1.00	
3	Root	0.5	1.76E-8		Root	0.3	9.02E-7	367.1
	Node 4	1.92	0.18	210.9	Node 3	1.6	0.97	
	Node 33	0.93	0.98		Node 34	0.17	1.00	
4	Root	0.45	21.78E-8		Root	0.26	4.94E-7	372.8
	Node 4	1.58	0.36	247.7	Node 3	1.28	0.97	
	node 33	0.07	0.99		Node 34	0.1	1.00	
5	Root	0.49	1.92E-7		Root	0.3	1.61E-6	369
	Node 4	2.02	0.12	209.2	Node 3	1.72	0.96	
	Node 33	1.02	0.97		Node 34	0.23	1.00	
6	Root	0.46	3.67E-7		Root	0.27	8.87E-7	380.4
	Node 4	1.58	5.64E-2	220.0	Node 3	1.26	0.97	
	Node 33	1.12E-5	1.0		Node 34	0.02	1.00	
7	Root	0.48	1.07E-8		Root	0.29	1.78E-8	371.6
	Node 4	1.95	1.07E-5	211.9	Node 3	1.67	0.96	
	Node 33	0.91	0.97		Node 34	0.19	1.00	
8	Root	0.42	2.49E-7		Root	0.25	6.46E-7	381.5
	Node 4	1.58	0.25	221.6	Node 3	1.29	0.97	
	Node 33	0.24	0.98		Node 34	0.24	1.00	

Only nodes where shifts of diversification rates have occurred are presented. In 31 of 32 trees two rate shifts were detected. In 23 trees the first shift is estimated to occur at node 3. In the remaining nine trees, the first shift is estimated to occur at node 4. The second shift occurs in 16 trees at node 33 and in 16 trees at node 34. r, speciation rates; ϵ , extinction rates.

Table S5. Additional information for each taxon (or close 16S rRNA relatives) that have been used in this study, as found in the literature

Taxon	Notes
<i>Acaryochloris</i> sp. JJ8A6*	BLAST result: <i>Aphanocapsa muscicola</i> 5N-04 (97%) is a unicellular cyanobacterium isolated from monumental fountains in Florence (Italy) (4).
<i>Anabaena</i> sp. PCC 7108	Strain PCC 7108 is a nontoxic, filamentous cyanobacterium capable of forming heterocysts, isolated from intertidal zone (United States) (7). BLAST result: <i>Anabaena</i> sp. KVSF7 (98%)
<i>Arthonema gygaxiana</i> UTCC 393	Strain UTCC 393 is filamentous, isolated from lake of Bays Twnsp., Ontario (Canada) (8). BLAST result: <i>Pseudanabaena</i> sp. 1tu24s9 (98%)
<i>Arthrosphaera platensis</i> PCC 8005	Strain PCC 8005 is a filamentous cyanobacteria not forming heterocysts, usually found in alkaline lakes (11). BLAST result: <i>Spirulina maxima</i> UTEX "LB 2342" (99%)
<i>Calothrix</i> sp. PCC 7103	Strain PCC 7103 is a filamentous cyanobacterium able to form heterocysts (basal end) and akinetes (19). BLAST result: <i>Calothrix desertica</i> PCC 7102 (99%)
<i>Chamaesiphon subglobosus</i> PCC 7430	Strain PCC 7430 has been described as unicellular cyanobacterium that reproduces by successive unequal binary fission and occurs in freshwater (20). BLAST result: <i>Chamaesiphon minutus</i> (98%)
<i>Chlorogloeopsis</i> sp. PCC 7518	Strain PCC 7518 is a multicellular, thermophilic cyanobacterium that lacks branching patterns. Additionally, strain PCC 7518 has lost the ability to form heterocysts (21). BLAST result: <i>Chlorogloeopsis</i> sp. Greenland_2 (99%)
<i>Chroococcidiopsis</i> sp. CC2	Strain CC2 is a hypolithic cyanobacterium isolated from enrichment cultures, which have been originally sampled from hyperarid deserts in China (22). BLAST result: <i>Chroococcidiopsis</i> sp. CC3 (99%)
<i>Chroococcus</i> sp. JJCM*	BLAST result: <i>Chroococcus</i> sp. 2T05h (97%) is a unicellular bacterium isolated from fountains in Italy and Spain (4).
<i>Crinalium magnum</i> SAG 34.87*	BLAST result: <i>Crinalium epipsammum</i> SAG 22.89 (100%) is a filamentous cyanobacterium with elliptical trichomes (24)
Cyanobacterium G40 (present study)	Strain G40 is a marine, filamentous cyanobacterium with cell differentiation; isolated from North sea (The Netherlands). BLAST result: <i>Nodularia spumigena</i> (95%)
<i>Cyanobium</i> sp. JJ23-1*	BLAST result: <i>Synechococcus</i> sp. BO 8805 (99%) is a unicellular, phycocyanin rich isolate from Lake Constance (16)
<i>Cyanothece</i> sp. PCC 8801	Strain PCC 8801 is a unicellular, nitrogen-fixing cyanobacterium without sheath, originally named " <i>Synechococcus</i> " RF-1 (25). BLAST result: <i>Cyanothece</i> sp. PCC 8802 (99%)
<i>Dactylococcopsis salina</i> PCC 8305	Strain PCC 8305 is a unicellular, halophilic cyanobacterium with fusiform, often elongated cells growing (26). BLAST result: <i>Cyanothece</i> sp. 104 (99%)
<i>Dermocarpa</i> sp. MBIC10768	BLAST result: <i>Stanieria</i> PCC 7301 (98%) is a unicellular cyanobacterium able to form baeocysts (9)
<i>Dermocarpea</i> "incrassata" SAG 29.84	Strain SAG 29.84 (PCC 7326) is a unicellular marine cyanobacterium isolated from snail shell, Puerto Penasco (Mexico) and the only axenic representative (27). BLAST result: <i>Myxosarcina</i> sp. PCC 7312 (96%)
<i>Filamentous thermophilic cyanobacterium</i> tBTRCCn 301	Cyanobacterium tBTRCCn 301 is a filamentous cyanobacterium of unknown affiliation isolated from thermal springs close to the dead sea (Jordan) (29, 30). BLAST result: <i>Synechococcus</i> sp. C9 (92%)
<i>Fischerella muscicola</i> PCC 7414	Strain PCC 7414 is a filamentous, heterocystous cyanobacterium with uniserate branches composed of longer cells (12, 20). BLAST result: <i>Fischerella muscicola</i> (99%)
<i>Geitlerinema</i> sp. BBD HS217	Strain BBD HS217 is a gliding, filamentous, nonheterocystous cyanobacteria (32). Trichomes of Geitlerinema are generally described as straight or slightly sinuous (20). BLAST result: <i>Geitlerinema</i> sp. BBD_P2b-1 (99%)
<i>Gloebacter violaceus</i> PCC 7421	Strain PCC 7421 is a rod-shaped, unicellular cyanobacterium lacking thylacoid membranes, isolated from calcareous rock, Switzerland (33). BLAST result: <i>Gloebacter violaceus</i> VP3-01 (99%)
<i>Gloeothece</i> sp. PCC 6909	Strain PCC 6909 is a unicellular, rod-shaped cyanobacterium capable of nitrogen fixation, isolated from freshwater (20). BLAST result: <i>Gloeothece membranacea</i> (99%)
<i>Halospirulina tapeticola</i> CCC Baja-95 Cl.2	Strain CCC Baja-95 Cl.2 is a highly halotolerant, filamentous cyanobacterium with helically coiled trichomes (35). BLAST result: <i>Halospirulina</i> sp. CCC Baja-95 Cl.3 (99%)
<i>Leptolyngbya</i> sp. ANT.L52.1	Strain ANT.L52.1 is a filamentous cyanobacterium with sheath (36). BLAST result: <i>Phormidium priestleyi</i> ANT.LPR2.6 (98%)
<i>Lyngbya aestuarii</i> PCC 7419	Strain PCC 7419 is a filamentous cyanobacterium without cell differentiation that is capable of nitrogen fixation (12). BLAST result: <i>Lyngbya aestuarii</i> (99%)
<i>Microcoleus chthonoplastes</i> PCC 7420	Strain PCC 7420 is a filamentous, nonheterocystous cyanobacterium collected from salt marsh at Woods Hole, MA. Trichomes often parallel surrounded by common homogenous sheath (20, 38). BLAST result: <i>Microcoleus chthonoplastes</i> NCR (99%)
<i>Microcystis aeruginosa</i> strain 038*	BLAST result: <i>Microcystis aeruginosa</i> VN441 (99%) is a unicellular, coccoid cyanobacterium, which produces microcystin, isolated from ponds in Vietnam (23).
<i>Myxosarcina</i> sp. PCC 7312	Strain PCC 7312 is a unicellular cyanobacterium, morphologically indistinguishable from <i>Chroococcidiopsis</i> . Isolated from a snail shell, Puerto Penasco, Mexico (27). BLAST result: <i>Pleurocapsa</i> sp. PCC 7314 (99%)

Table S5. Cont.

Taxon	Notes
<i>Myxosarcina</i> sp. PCC 7325	Description of PCC 7325 is the same as for <i>Myxosarcina</i> sp. PCC 7312 (27). BLAST result: <i>Myxosarcina</i> sp. PCC 7312 (96%)
<i>Nodularia "sphaerocarpa"</i> PCC 7804	Strain PCC 7804 is a toxic, filamentous, heterocystous strain isolated from thermal spring (southern France) (20, 31). BLAST result: <i>Nodularia sphaerocarpa</i> BECID 36 (99%)
<i>Nostoc</i> sp. PCC 7120	Strain PCC 7120 is a filamentous cyanobacterium capable of forming heterocysts (39). BLAST result: <i>Anabaena</i> sp. CCAP 1403/4A (98%)
<i>Oscillatoria sancta</i> PCC 7515	Strain PCC 7515 is a filamentous, nonheterocystous cyanobacterium isolated from a greenhouse water tank, Stockholm, Sweden. Capable of aerobic nitrogen fixation (5, 20). BLAST result: <i>Oscillatoria sancta</i> (99%)
" <i>Oscillatoria</i> " sp. IW19	Strain IW19 is a filamentous isolate from Lake Loosdrecht. Originally, termed " <i>Oscillatoria limnetica</i> -like" (41). BLAST result: <i>Leptolyngbya</i> sp. OBB30502 (97%)
" <i>Phormidium mucicola</i> " IAM M-221	Strain M-221 is a filamentous, nonheterocystous cyanobacterium (10). BLAST result: <i>Pseudanabaena</i> PCC7403 (99%)
" <i>Planktothrix</i> " sp. FP1	Strain FP1 is a filamentous, nonheterocystous cyanobacterium, isolated from Lake Varese, Italy (37). BLAST result: <i>Limnothrix redekei</i> 2LT25S01 (99%)
" <i>Plectonema</i> " sp. F3	Strain F3 is a filamentous cyanobacterium with false branching. It is a marine, nonpolar cyanobacterial strain (36). BLAST result: <i>Leptolyngbya</i> sp. ANT.L52.1 (97%)
<i>Pleurocapsa</i> sp. CALU 1126*	BLAST result: <i>Pleurocapsa minor</i> SAG 4.99 (98%) is a unicellular, hypolithic cyanobacterium isolated from a quartz pebble, Namib desert, Namibia (27)
<i>Pleurocapsa</i> sp. PCC 7516	Strain PCC 7516 is a unicellular, marine cyanobacterium isolated from a rock chip, Marseille, France (20, 28). BLAST result: <i>Myxosarcina</i> sp. PCC 7312 (97%)
<i>Prochlorococcus</i> sp. MIT9313	Strain MIT9313 is a low-light adapted, unicellular cyanobacterium isolated from Gulf Stream water samples (15). BLAST result: <i>Prochlorococcus</i> sp. MIT9303 (99%)
<i>Prochloron</i> sp.	<i>Prochloron</i> sp. is a unicellular, spherical shaped symbiont of marine ascidians lacking Phycobilisomes (42). BLAST result: <i>Cyanothecae</i> sp. PCC 8802 (93%)
<i>Prochlorothrix hollandica</i>	This is a filamentous cyanobacterium isolated from Lake Loosdrecht, Netherlands (18). BLAST result: <i>Prochlorothrix hollandica</i> SAG 10.89 (99%)
<i>Pseudanabaena</i> sp. PCC 7304	Strain PCC 7304 is a filamentous cyanobacterium belonging to the <i>Pseudanabaena</i> cluster (9). BLAST result: <i>Phormidium mucicola</i> AM M-221 (99%)
<i>Pseudanabaena</i> sp. PCC 6802	Strain PCC 6802 is a filamentous cyanobacterium belonging to the <i>Pseudanabaena</i> cluster (9). BLAST result: <i>Pseudanabaena</i> sp. 1a-03 (95%)
<i>Radiocystis</i> sp. JJ30-3*	BLAST result: <i>Synechocystis</i> sp. PCC 6803 (100%) is a unicellular cyanobacterium isolated from freshwater, California (20, 43)
<i>Scytonema</i> sp. U-3-3*	BLAST result: <i>Scytonema hofmanni</i> PCC 7110 (95%) is a filamentous heterocystous cyanobacterium with sheath, isolated from limestone, Crystal Cave, Bermuda (38)
<i>Spirulina</i> sp. PCC 6313	Strain PCC 6313 was isolated from brackish water, California. It is a filamentous, loosely coiled cyanobacterium (20, 38). BLAST result: <i>Spirulina major</i> OBB36S18 (99%)
<i>Starria zimbabweensis</i> SAG 74.90	<i>Starria</i> is a nonbranching, filamentous cyanobacterium with triradiate trichomes (20). BLAST result: <i>Crinalium magnum</i> SAG 34.87 (97%)
<i>Sympytonema</i> sp. 1517	Strain 1517 is a filamentous, heterocystous cyanobacterium showing mainly Y-branching, isolated from Soil, Papua New Guinea (44). BLAST result: <i>Sympytonema</i> sp. 1269-1(100%)
<i>Symploca</i> sp. PCC 8002	Strain PCC 8002 is a filamentous, nonheterocystous cyanobacterium isolated from high intertidal zones, North Wales (9, 20). BLAST result: <i>Symploca</i> sp. HBC5 (97%)
<i>Synechococcus</i> lividus C1	Strain C1 is a thermophilic, unicellular cyanobacterium, a part of the "unicellular-thermophilic" (UNIT) sequence group (5). BLAST result: <i>Synechococcus</i> sp. Strain PCC 6717 (99%)
<i>Synechococcus</i> sp. WH8101	Strain WH8101 is a unicellular, facultatively marine cyanobacterial strain that lacks phycerythrin (14). BLAST result: <i>Synechococcus</i> sp. RS9909 (99%)
<i>Synechococcus</i> sp. CC9605	Strain CC9605 is a marine, unicellular cyanobacterium isolated from California current (13). BLAST result: <i>Synechococcus</i> sp. WH 8109 (99%)
<i>Synechococcus</i> sp. C9	Strain C9 is a unicellular cyanobacterium, part of the <i>Gloeobacter</i> (GBACT) group estimated to be close to the root of cyanobacteria (5). BLAST result: <i>Candidatus Gloeomargarita lithophora</i> D10 (98%)
<i>Synechococcus elongatus</i> PCC 6301	Strain PCC 6301 is a unicellular, rod-shaped cyanobacterium that occurs in freshwater (17). BLAST result: <i>Synechococcus elongatus</i> PCC 7942 (100%)
<i>Synechocystis</i> sp. PCC 6803	Strain PCC 6803 is a unicellular cyanobacterium isolated from freshwater, California (20, 43). BLAST result: <i>Synechocystis</i> sp. PCC 6714 (100%)
<i>Synechococcus</i> sp. P1	Strain P1 is a unicellular cyanobacterium, part of the <i>Gloeobacter</i> (GBACT) group which has been estimated to be close to the root of the cyanobacterial line (5). BLAST result: <i>Synechococcus</i> sp. P2 (100%)

Table S5. Cont.

Taxon	Notes
<i>Synechocystis</i> sp. PCC 6308	Strain PCC 6308 is a unicellular cyanobacterium isolated from lake water, WI (20). BLAST result: <i>Synechocystis</i> sp. VNM-13-10 (98%)
<i>Thermosynechococcus elongatus</i> BP-1	Strain BP-1 is a thermophilic, rod-shaped, unicellular cyanobacterium originally isolated from a hot spring in Beppu (Japan) (6). BLAST result: <i>Synechococcus elongatus</i> (100%)
<i>Trichodesmium erythraeum</i> IMS 101	Strain IMS101 is a marine, filamentous cyanobacterium capable of aerobic nitrogen fixation without heterocyst formation (40). BLAST result: <i>Trichodesmium</i> sp. (99%)

For each taxon a BLAST result is shown with the maximum identity given in brackets. Taxa with their names in quotes have likely been misidentified in the original publication considering their BLAST results.

*Citation for a close relative identified by BLAST search.

Dataset S1. Sequence alignment used for the phylogenetic-tree reconstruction

[Dataset S1](#)

Dataset S2. XML input files for the different analyses using a relaxed clock with lognormally distributed evolutionary rates

[Dataset S2](#)